

## Research Paper

# G protein subunit alpha i2's pivotal role in angiogenesis

Chao-wen Bai<sup>1#</sup>, Lu Lu<sup>2#</sup>, Jia-nan Zhang<sup>1#</sup>, Chengyu Zhou<sup>3#</sup>, Yi-chao Ni<sup>1#</sup>, Ke-ran Li<sup>4</sup>, Jin Yao<sup>4✉</sup>, Xiao-zhong Zhou<sup>1✉</sup>, Chang-gong Lan<sup>2✉</sup> and Cong Cao<sup>1✉</sup>

1. Department of Orthopedics, Clinical Research Center of Neurological Disease, The Second Affiliated Hospital of Soochow University, Institution of Neuroscience, Soochow University, Suzhou, China.
2. Department of Joint Surgery and Geriatric Orthopedics, Affiliated Hospital of Youjiang Medical University for Nationalities, Guangxi Key Laboratory of Basic and Translational Research of Bone and Joint Degenerative Diseases, Guangxi Biomedical Materials Engineering Research Center for Bone and Joint Degenerative Diseases, Baise City, China.
3. Department of Neuroscience, Case Western Reserve University, Cleveland, USA.
4. The Fourth Medical School, Eye hospital, Nanjing Medical University, Nanjing, China.

# Equal contributors.

✉ Corresponding authors: Prof. Xiao-zhong Zhou (zhouxz@suda.edu.cn), Prof. Jin Yao (dryaojin@126.com), Prof. Chang-gong Lan (landlong120@sina.com) and Prof. Cong Cao (caocong@suda.edu.cn).

© The author(s). This is an open access article distributed under the terms of the Creative Commons Attribution License (<https://creativecommons.org/licenses/by/4.0/>). See <http://ivyspring.com/terms> for full terms and conditions.

Received: 2023.12.04; Accepted: 2024.02.26; Published: 2024.03.03

## Abstract

Here we explored the potential role of Gai2 (G protein subunit alpha i2) in endothelial cell function and angiogenesis.

**Methods:** Genetic methodologies such as shRNA, CRISPR/Cas9, dominant negative mutation, and overexpression were utilized to modify G  $\alpha$  i2 expression or regulate its function. Their effects on endothelial cell functions were assessed *in vitro*. *In vivo*, the endothelial-specific G  $\alpha$  i2 shRNA adeno-associated virus (AAV) was utilized to silence G  $\alpha$  i2 expression. The impact of this suppression on retinal angiogenesis in control mice and streptozotocin (STZ)-induced diabetic retinopathy (DR) mice was analyzed.

**Results:** Analysis of single-cell RNA sequencing data revealed *Gai2* (*GNAI2*) was predominantly expressed in retinal endothelial cells and expression was increased in retinal endothelial cells following oxygen-induced retinopathy (OIR) in mice. Moreover, transcriptome analysis linking *Gai2* to angiogenesis-related processes/pathways, supported by increased *Gai2* expression in experimental OIR mouse retinas, highlighted its possible role in angiogenesis. In various endothelial cell types, shRNA-induced silencing and CRISPR/Cas9-mediated knockout (KO) of Gai2 resulted in substantial reductions in cell proliferation, migration, invasion, and capillary tube formation. Conversely, Gai2 over-expression in endothelial cells induced pro-angiogenic activities, enhancing cell proliferation, migration, invasion, and capillary tube formation. Furthermore, our investigation revealed a crucial role of Gai2 in NFAT (nuclear factor of activated T cells) activation, as evidenced by the down-regulation of NFAT-luciferase reporter activity and pro-angiogenesis NFAT-targeted genes (*Egr3*, *CXCR7*, and *RND1*) in Gai2-silenced or -KO HUVECs, which were up-regulated in Gai2-overexpressing endothelial cells. Expression of a dominant negative Gai2 mutation (S48C) also down-regulated NFAT-targeted genes, slowing proliferation, migration, invasion, and capillary tube formation in HUVECs. Importantly, *in vivo* experiments revealed that endothelial Gai2 knockdown inhibited retinal angiogenesis in mice, with a concomitant down-regulation of NFAT-targeted genes in mouse retinal tissue. In contrast, Gai2 over-expression in endothelial cells enhanced retinal angiogenesis in mice. Single-cell RNA sequencing data confirmed increased levels of Gai2 specifically in retinal endothelial cells of mice with streptozotocin (STZ)-induced diabetic retinopathy (DR). Importantly, endothelial Gai2 silencing ameliorated retinal pathological angiogenesis in DR mice.

**Conclusion:** Our study highlights a critical role for Gai2 in NFAT activation, endothelial cell activation and angiogenesis, offering valuable insights into potential therapeutic strategies for modulating these processes.

## Introduction

Angiogenesis is a fundamental and vital physiological process in the body [1, 2], serving as a critical mechanism to uphold the body's stability, and the functionality of cells, tissues, and organs [3-6].

Vascular endothelial growth factor (VEGF) and other stimuli trigger the activation of existing vascular endothelial cells, often referred as “tip cells”. These specialized cells release proteases, facilitating the degradation of the basement membrane, thus enabling the detachment of endothelial cells from their original vessel walls [7]. Tip cells exhibit slow proliferation and extend numerous filopodia, effectively guiding the direction of the angiogenic process [3-6]. Detached endothelial cells subsequently proliferate and migrate into the surrounding matrix, coalescing to form sprouts that interconnect adjacent blood vessels [8]. Endothelial cells trailing behind the tip cells continue their proliferation, contributing to the development of new capillary buds and the intricate network of fresh blood vessels [3-6]. The intricate mechanisms governing the activation of endothelial cells and the process of angiogenesis remain largely unknown, serving as the primary research focus of our group [9-13].

G $\alpha$ i proteins (G protein  $\alpha$  i subunits), a subgroup of G protein family, are critical mediators of inhibitory signaling in the G protein-coupled receptor (GPCR) system [14-16]. Upon activation by GPCR binding, G $\alpha$ i proteins catalyze the exchange of GDP for GTP, leading to dissociation from the  $\beta\gamma$  subunits and subsequent downstream effects [14-16]. G $\alpha$ i proteins inhibit adenylyl cyclase (AC), resulting in decreased cyclic AMP (cAMP) levels, which impacts a wide range of cellular processes, including ion channel regulation and neurotransmitter release [14-16]. Additionally, G $\alpha$ i proteins modulate other signaling pathways, such as the MAPK (mitogen-activated protein kinase) and NFAT (nuclear factor of activated T cells) cascade, making them pivotal players in the regulation of diverse physiological processes and the focus of significant research and therapeutic interest [17]. Three primary G $\alpha$ i members are G $\alpha$ i1, G $\alpha$ i2 and G $\alpha$ i3 [18, 19].

Our group also established a pivotal role of G $\alpha$ i proteins in mediating signaling by receptor tyrosine kinases (RTKs) and other non-GPCR receptors. Following epidermal growth factor (EGF) stimulation, G $\alpha$ i1 and G $\alpha$ i3 form a complex with activated EGFR to mediate downstream adaptor protein association and Akt-mammalian target of rapamycin (mTOR) cascade activation [20]. G $\alpha$ i1 and G $\alpha$ i3 are also required for the signal transduction of other RTKs [10, 13, 21-23], including keratinocyte growth factor receptor (KGFR) [23], vascular endothelial growth factor receptor 2 (VEGFR2) [13], the BDNF receptor Tropomyosin receptor kinase B (TrkB) [22] and c-kit [10]. Moreover, several non-RTK receptors also require G $\alpha$ i1 and G $\alpha$ i3 for downstream signal transduction, including Netrin-1 receptor CD146

(Cluster of Differentiation 146) [11], lipopolysaccharide (LPS) receptor Toll-like receptor 4 (TLR4)-and CD14 [24] and IL-4 receptor IL-4R [25].

Recent investigations highlight the significant role of G $\alpha$ i2 protein in the proliferation of cancer cells [26, 27]. In a study by Chen *et al.*, G $\alpha$ i2 over-expression was identified as a pivotal factor in promoting the growth of hepatocellular carcinoma (HCC) cells [27]. Silencing or knockout (KO) of G $\alpha$ i2 led to mitochondrial dysfunction, apoptosis, and growth arrest in HCC cells, impeding HCC xenograft growth in nude mice [27]. Our recent study reported elevated G $\alpha$ i2 mRNA and protein expression in human gliomas, essential for *in vitro* and *in vivo* glioma cell growth [26]. Mechanistically, G $\alpha$ i2 enhanced the viability, proliferation, and mobility of human glioma cells, potentially through activation of the nuclear factor kappa B (NF- $\kappa$ B) pathway [26]. Nonetheless, the specific involvement of G $\alpha$ i2 in endothelial cell activation and angiogenesis, as well as the underlying mechanisms, have not been extensively studied to date.

## Methods

**Bioinformatics studies.** Analysis of publicly-available single-cell RNA sequencing (scRNA-seq) data from streptozotocin (STZ)-induced diabetic mice and oxygen-induced retinopathy (OIR) mice were conducted using data retrieved from the NCBI General Gene Expression Database (GEO) via GSE209872 and GSE150703. Initial processing of raw counts was performed using the R package Seurat (version 3.0), implementing quality control parameters such as minimum cells (min. cells = 3), minimum features (min. features = 100), and criteria for RNA features (nFeature\_RNA  $\geq$  300, nFeature\_RNA < 5000, mito.ratio < 0.20). Subsequently, identification of highly variable genes (top 5000) was executed via the FindVariableFeatures function. Principal component analysis (PCA) was applied to select the top 30 principal components for subsequent cluster analysis. Unsupervised hierarchical clustering, based on an appropriate resolution, was performed using the FindClusters function. Visualization of the clustered data was achieved through Uniform Manifold Approximation and Projection (UMAP) projections. Marker genes were identified, with additional markers of retinal cells retrieved from the GeneCards database to classify each cluster. Visualization of G $\alpha$ i2 location and expression was accomplished using a density plot. Differential gene expression analysis was conducted to identify genes exhibiting up-regulated ( $P$  value < 0.05 and avg\_log2FC > 0.25) and down-regulated ( $P$  value < 0.05 and avg\_log2FC < -0.25) expression specifically in

endothelial cells. Visualization of these findings was achieved using a volcano plot. Furthermore, publicly available transcriptome sequencing data for oxygen-induced retinopathy (OIR) mice were obtained from GEO using the search code GSE200195. Correlation analysis was conducted to determine genes most correlated with *Gai2*. The top 100 correlated genes were subjected to enrichment analysis using The Database for Annotation, Visualization, and Integrated Discovery (DAVID). Pathways were ranked by *P*-value, and the top 12 biological processes (BP) and KEGG (Kyoto Encyclopedia of Genes and Genomes) pathways were visualized using the ggplot2 package.

**Chemicals and reagents.** Polybrene, puromycin, ionomycin, cyclosporin A (CsA), and other chemicals were provided by Sigma-Aldrich (St. Louis, MO) unless otherwise specified. All antibodies were described in our previous studies [9–12, 26]. Fluorescence dyes were provided by Thermo-Fisher Invitrogen (Soochow, China). All viral constructs and verified mRNA primers were supplied by Genechem (Shanghai, China).

**Cells.** The culture of various endothelial cell types in this study, including human umbilical vein endothelial cells (HUVECs), human microvascular endothelial cells (hRMECs), and human cerebral microvascular endothelial cells (hCMECs), was reported in our previous publications [9–12]. Endothelial cells were cultured in DMEM/F-12 medium with high glucose and 10% FBS (Gibco, Suzhou, China), 5 µg/mL insulin, 5 µg/mL EGF, 5 ng/mL VEGF, and 24 µg/mL adenine, maintain a pro-angiogenic active state [12], and their genotype have been authenticated through short tandem repeat (STR) analysis, population doubling time assessments, and morphological examinations.

***Gai2* small hairpin RNA (shRNA).** The lentiviral GV369 (Ubi-MCS-SV40-IRES-puromycin) construct (no tag) containing puromycin selection gene was reported in our previous studies [9, 12]. It was utilized for shRNA experiment. Briefly, *Gai2* shRNA sequence was first inserted into the lentiviral construct. The latter, together with packaging vectors pHelper 1.0 and pHelper 2.0 (Genechem), were co-transduced to HEK-293 cells, thereby generating lentivirus. The virus, at MOI (multiplicity of infection) of 10, was added to cultured endothelial cells. Puromycin-containing complete medium was thereafter added to the cultured endothelial cells and stable cells were formed after 5–6 passages. Knockdown of *Gai2* in endothelial cells was verified at both mRNA and protein levels. Control cells were treated with scramble control scramble shRNA [26]. In the context of *in vivo* studies, the mouse *Gai2* shRNA sequence

was incorporated into an adeno-associated virus 5 (AAV5)-TIE1 construct [12], featuring the endothelial-specific promoter sequence of TIE1 (Genechem, Shanghai, China). Subsequently, the construct was transfected into HEK-293 cells to produce AAV, which was then administered to mice via intravitreal injection.

***Gai2* knockout (KO).** The CRISPR-associated 9 (Cas9)-expressing stable HUVECs, reported in our previous studies [9, 12], were transduced with the previously-reported [26] lentivirus-packed CRISPR/Cas9-*Gai2*-KO construct (containing puromycin selection gene). HUVECs were then selected by puromycin and distributed into 96-well plates. The stable cells were then subject to *Gai2* KO verification and thereafter single stable *Gai2* KO HUVECs (“ko*Gai2*”) were formed. Control Cas9-expressing HUVECs were transduced with lentivirus-packed CRISPR/Cas9-KO construct containing scramble sgRNA sequence (“Cas9”). The same CRISPR/Cas9 procedures were employed to other endothelial cells (hRMECs and hCMEC/D3) to deplete *Gai2*.

***Gai2* over-expression and dominant negative mutation.** The lentivirus packed *Gai2*-overexpressing GV369 construct was reported in our previous study [26] and was added to cultured endothelial cells. Puromycin-containing complete medium was thereafter added to the cultured endothelial cells, and stable cells formed after 5–6 passages. *Gai2* over-expression in the selected stable endothelial cells was verified at both mRNA and protein levels. Control cells were stably transduced with the empty GV369 vector (“Vec”). A site-directed mutagenesis (Genechem) using targeted primers was employed to generate the dominant negative S48C *Gai2* cDNA [28], and it was verified through DNA sequencing to confirm the presence of the desired mutation. The sequence was inserted into the GV369 construct, and the latter was stably transduced to endothelial cells. For *in vivo* studies, the *Gai2* cDNA sequence was introduced into the AAV5-TIE1 construct. It was then transfected into HEK-293 cells to generate AAV, which was subsequently administered to mice via intravitreal injection.

**Cellular assays.** Cellular functional assays, including the assessment of cell proliferation through EdU (5-ethynyl-2'-deoxyuridine) staining of cell nuclei, “Transwell” *in vitro* cell migration and “Matrigel Transwell” *in vitro* cell invasion, *in vitro* capillary tube formation, nuclear TUNEL staining assay, JC-1 staining of mitochondrial depolarization the Caspase-3 and the Caspase-9 activity assays were described early [12, 13, 29–31]. qRT-PCR (quantitative reverse transcription polymerase chain reaction) and Western blotting assays have been previously detailed



in earlier publications [20, 32, 33]. For "Transwell" and "Matrigel Transwell" assays, precisely  $1.5 \times 10^4$  cells with specific genetic treatments were added into each chamber. In the capillary tube formation assay,  $0.75 \times 10^5$  cells per well were seeded onto pre-coated 24-well plates. For EdU, JC-1 and TUNEL staining assays,  $5 \times 10^4$  cells per well were seeded into 24-well plates. Crystal violet dye was utilized to stain the migrated/invaded cells. In cases where different proteins needed examination within the same set of lysates, parallel "sister" gels were employed. All the mRNA primers and viral constructs were sourced from Genechem (Shanghai, China). Figure S1 included the uncropped blotting images of the study.

**NFAT-luciferase reporter assay.** HUVECs were transduced with a NFAT-luciferase reporter construct (Genechem), and stable cells were established after puromycin selection. Cells were then subjected to described treatments, and a luciferase assay was conducted, measuring both firefly luciferase (NFAT reporter) and Renilla luciferase (control) activities through the ONE-Glo™ Luciferase Assay System (Promega, Suzhou, China). The data was analyzed by normalizing firefly luciferase activity to Renilla luciferase activity.

**Animal models, virus injection in mouse retina and retinal staining.** The intravitreal injection of AAV involved adult C57BL/6 mice from the SLAC Laboratory Animal Center (Shanghai, China). These mice were housed in a clean specific pathogen-free (SPF) animal facility, maintained at a temperature of  $24 \pm 1^\circ\text{C}$ , with a 12-hour light and dark cycle, and provided with free access to water and food. Anesthesia was induced as previously described [12], and a 33-gauge disposable needle was inserted through the sclera at the equator and posterior to the limbus, directly into the vitreous cavity. Approximately 0.1  $\mu\text{L}$  of AAV was then injected into the vitreous cavity, targeting the needle above the optic nerve head. Twenty-one days after virus injection, the isolectin B4 (IB4) staining of retinal vasculature and NeuN (neuronal nuclear antigen) immunofluorescence staining of retinal ganglion cells (RGCs) were performed using the previously-described protocols [9–11]. For the establishment of oxygen-induced retinopathy (OIR) mouse model, a previously-described method was utilized [13]. Briefly, newborn C57BL/6 mice at P7 along with their nursing mothers were subjected to 75% oxygen exposure using a BioSpherix oxycycler (BioSpherix, Lacona, NY) for five days, followed by another five days of returning to room air. For the establishment of diabetic retinopathy (DR) animal model, C57B/6J mice, aged 4–5 weeks, underwent an overnight fasting period with unrestricted access to water. The

subsequent day, the mice were administered intraperitoneally with freshly prepared streptozotocin (STZ) at a dosage of 60 mg/kg, dissolved in cold 100 mM pH 4.5 citrate buffer (Sigma-Aldrich), for five consecutive days. One week following the final STZ injection, tail vein blood glucose levels were evaluated. Mice displaying fasting blood glucose levels surpassing 300 mg/dL (16.6 mmol/L) were classified as diabetic and included in subsequent investigations. The "Mock" mice were administered citrate buffer injections. The assessment of retinal vascular leakage through Evans blue (EB) staining had also been previously outlined [12, 34]. To isolate GFP-positive retinal endothelial cells from mouse retina, mice were sacrificed. Their eyes were carefully dissected to extract the retina. The tissues were then enzymatically digested via Collagenase I and Trypsin (Sigma) to obtain single-cell suspensions. Following digestion, cells were passed through a 70- $\mu\text{m}$  Falcon cell strainer (Corning, Shanghai, China) and were centrifuged carefully. GFP-positive endothelial cells were then isolated using fluorescence-activated cell sorting (FACS) via BD FACSaria machine (BD, Shanghai, China). The isolated cells were then cultured into above mentioned medium. All animal protocols adhered to the guidelines established by the Institutional Animal Care and Use Committee and the Ethic Committee of Soochow University, in accordance with the provisions outlined in the ARVO (Association for Research in Vision and Ophthalmology) statement.

**Statistical analyses.** Statistical analyses were performed on normally-distributed data, presented as means  $\pm$  standard deviation (SD). To assess significance, we employed one-way ANOVA followed by Scheffe's f-test for comparisons involving three or more groups, using SPSS 23.0, or the two-tailed unpaired t-test for comparisons between two groups, using Excel 2007. Statistical significance was defined as *P*-values below 0.05.

## Results

### Gai2 is highly expressed in endothelial cells and participates in angiogenesis and signaling

Among the models employed to investigate abnormal angiogenesis, oxygen-induced retinopathy (OIR) is a well-established experimental system [35, 36]. The manipulation of oxygen levels in the OIR model induces a state of retinal ischemia followed by hyperoxia, resulting in the dysregulation of pro-angiogenic and anti-angiogenic factors. This imbalance triggers a cascade of molecular events, including the upregulation of vascular endothelial growth factor (VEGF), hypoxia-inducible factor (HIF),



and various cytokines and growth factors, culminating in the formation of abnormal blood vessels in the retina [35, 36]. Cellular responses such as endothelial cell proliferation, migration, and vascular remodeling contribute to the angiogenic process in OIR [35, 36].

We first conducted an analysis of publicly accessible single-cell RNA (scRNA) sequencing data (GEO: #GSE150703) comparing OIR mice and normoxic mice (NORM). The aim was to explore the cellular localization of *Gai2* (*GNAI2*) within the retina. Through dimensionality reduction, clustering, and annotation techniques, we categorized individual cells from the entire retina into 12 distinct clusters (Figure 1A). Subsequently, we utilized Uniform Manifold Approximation and Projection (UMAP) projections to visualize these clusters (Figure 1A). As depicted in Figure 1B, *Gai2* is ubiquitously expressed across all cell types within the mouse retina, with significantly elevated levels observed within endothelial cells. This suggests a potentially functional role for *Gai2* in endothelial cells. Furthermore, *Gai2* expression in pericytes and Müller glia is also relatively high compared to other cell types (Figure 1B). A volcano plot depicting the differential gene expression was generated comparing OIR and NORM mice groups that revealed a significant

up-regulation of *Gai2* (Figure 1C) specifically within retinal endothelial cells of the OIR group.

Next, we performed correlation analysis using publicly accessible transcriptome sequencing data (GEO: #GSE200195) from retinal tissue of OIR model mice to uncover genes co-expressed with *Gai2*. The top 100 co-expressing genes (CEGs) exhibiting the closest correlation were subjected to enrichment analysis, revealing the top 12 potential biological processes (BPs) in which *Gai2* might be involved. The analysis highlighted that *Gai2* CEGs were enriched in key biological processes for angiogenesis, including "Angiogenesis", "Cell migration", "Cell adhesion" and "Cell proliferation" (Figure 1D). The Kyoto Encyclopedia of Genes and Genomes (KEGG) analyses conducted on *Gai2* CEGs also revealed the top 12 pathways (Figure 1E). Among these pathways, several are recognized for their significance in endothelial cell activation and angiogenesis, including "Focal adhesion", "ECM-receptor interaction" and "Pathways in cancer" (Figure 1E).

To validate the above bioinformatics results, a previously-described OIR mouse model was utilized [13]. P2 mice were anesthetized and a 33-gauge needle was inserted through the sclera into the vitreous cavity, where 0.1  $\mu$ L of AAV5-TIE1-GFP was injected above the optic nerve head [12]. P7 mice were then

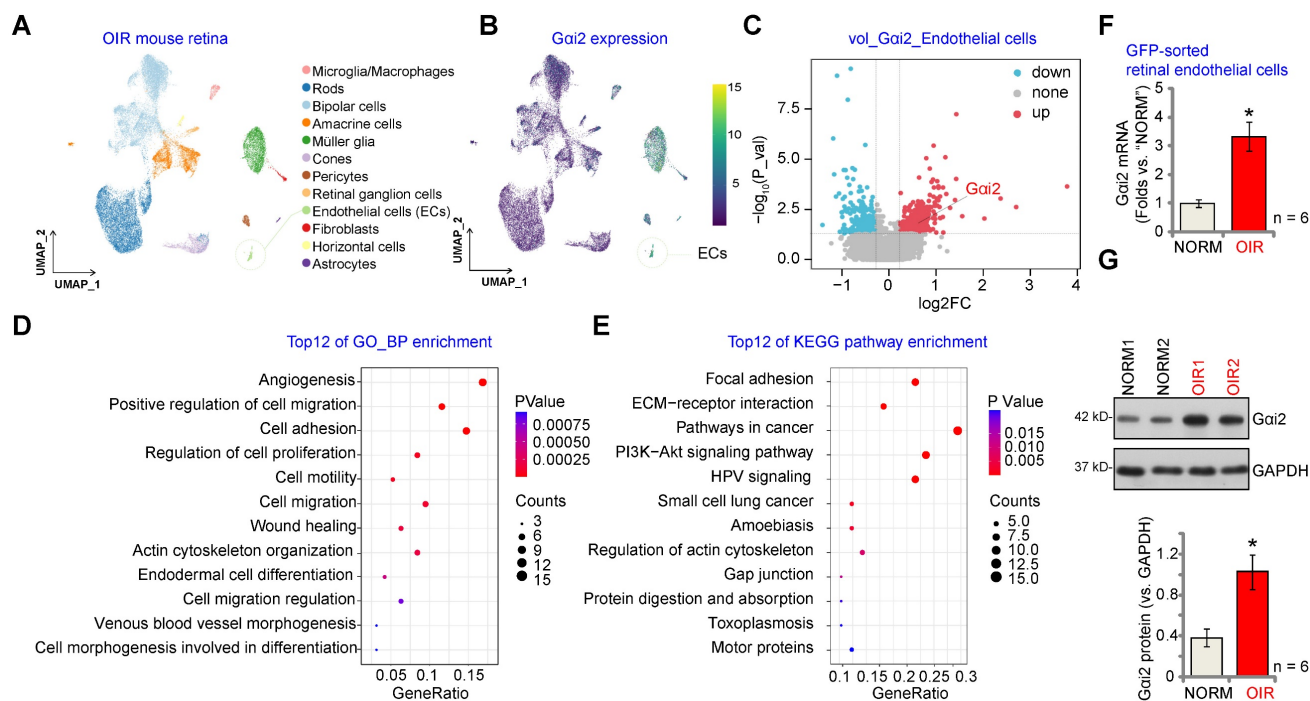


**Figure 1. *Gai2* is highly expressed in endothelial cells and participates in angiogenesis and signaling.** Visualization of the publicly available retinal scRNA-seq data (GEO: #GSE150703) of oxygen-induced retinopathy mice (OIR) and normoxic mice (NORM) using Uniform Manifold Approximation and Projection (UMAP) projections (**A**). The density plot illustrates the expression and spatial distribution of *Gai2* in retinas, with the scale of expression density displayed on the right side of the plot (**B**). A differential gene volcano plot of endothelial cells compares differences between OIR and NORM group (**C**). Enrichment analysis shown possible biological process (BP, **D**) and KEGG pathways (**E**) of the top 100 co-expressing genes (CEGs) with *Gai2* in retinal tissues of OIR model mice. Expression of *Gai2* mRNA (**F**) and protein (**G**) in GFP-sorted retinal cells of OIR mice and normoxic mice (NORM) mice was shown. Data were expressed as mean  $\pm$  standard deviation (SD). Each group included six mice (n = 6, half male, half female) (**F** and **G**). \* $P < 0.05$  versus "NORM" group.

subjected to 75% oxygen exposure for five days, followed by five days at room air. At P17, OIR or mock control mice were sacrificed to extract retinas, which were enzymatically digested and passed through a 70- $\mu$ m cell strainer before GFP-positive endothelial cells were sorted using FACS. These cells were then cultured. As demonstrated, *Gai2* mRNA (Figure 1F) and protein (Figure 1G) expression levels were notably elevated in GFP-positive endothelial cells of OIR mice compared to those from the mock control mice.

### **Gai2 silencing impedes *in vitro* angiogenesis in cultured endothelial cells**

Aiming to understand the potential role of *Gai2* in angiogenesis, we first employed a lentiviral shRNA method to silence *Gai2*. A set of three different lentivirus-packed shRNAs, sh*Gai2*-Sq1, sh*Gai2*-Sq2 and sh*Gai2*-Sq3 (with non-overlapping sequences), were separately transduced into cultured HUVECs, and stable cells formed after puromycin-based selection. As compared to the parental control ("Pare") HUVECs and scramble shRNA ("shC")-expressing HUVECs, *Gai2* mRNA (Figure 2A) and protein (Figure 2B) expression was substantially decreased in stable HUVECs with the described *Gai2* shRNAs. The mRNA and protein expression of two other members of the *Gai* family, *Gai1* and *Gai3*, was however not significantly altered in sh*Gai2* HUVECs (Figure 2A and B). Importantly, *Gai2* shRNA impeded HUVEC proliferation *in vitro* and decreased the percentage of EdU-positive nuclei (Figure 2C). "Transwell" assay results demonstrated that *in vitro* migration (Figure 2D) was slowed after *Gai2* silencing in HUVECs. Moreover, capillary tube formation was inhibited after shRNA-induced knockdown of *Gai2* (Figure 2E). These results demonstrate that *Gai2* silencing impedes *in vitro* angiogenesis in HUVECs. The shC control failed to alter proliferation (Figure 2C) migration (Figure 2D) and capillary tube formation (Figure 2E) in HUVECs.

To silence *Gai2* in other endothelial cell types, including human retinal microvascular endothelial cells (hRMECs) and human cerebral microvascular endothelial cells (hCMEC/D3) [12], the lentivirus-packed sh*Gai2*-Sq1 was transduced and stable cells established following puromycin selection. As compared to the endothelial cells with shC, *Gai2* mRNA expression was dramatically decreased in sh*Gai2*-Sq1-expressing hRMECs and hCMEC/D3 (Figure 2F). Importantly, *in vitro* cell proliferation (nuclear EdU incorporation, Figure 2G), migration (Figure 2H) and capillary tube formation (Figure 2I) were inhibited following *Gai2* silencing in hRMECs and hCMEC/D3. These results further support the

pro-angiogenic activity *Gai2 in vitro*.

### **Gai2 silencing provokes apoptosis in cultured endothelial cells**

We next examined whether *Gai2* silencing would provoke apoptosis in endothelial cells. As shown in cultured HUVECs, *Gai2* silencing by lentiviral sh*Gai2*-Sq1, sh*Gai2*-Sq2 or sh*Gai2*-Sq3 (see Figure 1), increased Caspase-3 (Figure 3A) and Caspase-9 activity (Figure 3B). Additionally, we observed enhanced cleavage of Caspase-3 and Poly(ADP-ribose) polymerase 1 (PARP) in sh*Gai2* HUVECs (Figure 3C). Silencing of *Gai2* in HUVECs also led to mitochondrial depolarization, as evidenced by the aggregation of JC-1 green monomers (Figure 3D), a characteristic indicator of mitochondrial apoptotic pathway activation [37]. *Gai2* silencing induced a moderate yet significant level of apoptosis in cultured HUVECs, as indicated by an approximately threefold increase in the percentage of TUNEL-positive nuclei in cells expressing sh*Gai2*-Sq1, sh*Gai2*-Sq2, or sh*Gai2*-Sq3 (Figure 3E). In other endothelial cell types, hRMECs and hCMEC/D3, *Gai2* silencing using sh*Gai2*-Sq1 (see Figure 1) similarly induced mitochondrial depolarization (Figure 3F) and apoptosis, as assessed by the increased ratio of TUNEL-positive nuclei (Figure 3G).

### **Complete Gai2 knockout (KO) leads to significant anti-angiogenic activity in cultured endothelial cells**

The results presented above demonstrate that silencing *Gai2* using shRNA inhibits *in vitro* angiogenesis in cultured endothelial cells. To rule out any potential off-target effects of the shRNAs and to achieve complete *Gai2* depletion, we employed the CRISPR/Cas9 strategy. Specifically, Cas9-expressing HUVECs, as described in our earlier publications [9-11], were transduced with a lentivirus-packed CRISPR/Cas9-*Gai2*-KO construct [26], which included a sequence of sgRNA targeting human *Gai2*. Subsequently, we established single stable *Gai2* KO HUVECs, referred to as "ko*Gai2*," following puromycin selection and verification of *Gai2* KO. As a control treatment, Cas9-expressing HUVECs were transduced with a lentivirus-packed CRISPR/Cas9-KO construct containing a scramble sgRNA sequence, denoted as "Cas9."

*Gai2* mRNA expression, as well as protein expression was effectively depleted in ko*Gai2* HUVECs (Figure 4A and B), while *Gai1* and *Gai3* expression remained unaffected (Figure 4A and B). *Gai2* KO in HUVECs induced a strong anti-angiogenic effect, significantly inhibiting *in vitro* cell proliferation (as indicated by nuclear EdU incorpo-

ration, Figure 4C), migration (Figure 4D), invasion (Figure 4E), and capillary tube formation (Figure 4F). Furthermore, Gai2 KO led to mitochondrial depolarization and the aggregation of JC-1 green monomers in HUVECs (Figure 4G). Increased TUNEL-nuclei staining provided further evidence of apoptosis activation in Gai2 KO HUVECs (Figure 4H). In both hRMECs and hCMEC/D3, Gai2 KO was achieved using the same CRISPR/Cas9 strategy (Figure 4I), resulting in impaired *in vitro* angiogenesis and reduced cell proliferation (nuclear EdU incorporation, Figure 4J), migration (Figure 4K), and capillary tube formation (Figure 4L).

## Gai2 over-expression promotes angiogenesis in cultured endothelial cells

Given that silencing or KO of Gai2 results in anti-angiogenic activity, we hypothesized that elevating Gai2 expression could enhance angiogenesis in cultured endothelial cells. To investigate this hypothesis, we transduced HUVECs with a lentivirus-packed Gai2-overexpressing construct known as "oeGai2" [26], and two stable cell lines, oeGai2-Slc1 and oeGai2-Slc2, were established through selection. In comparison to cells transfected with the vector control ("Vec"), the oeGai2-expressing

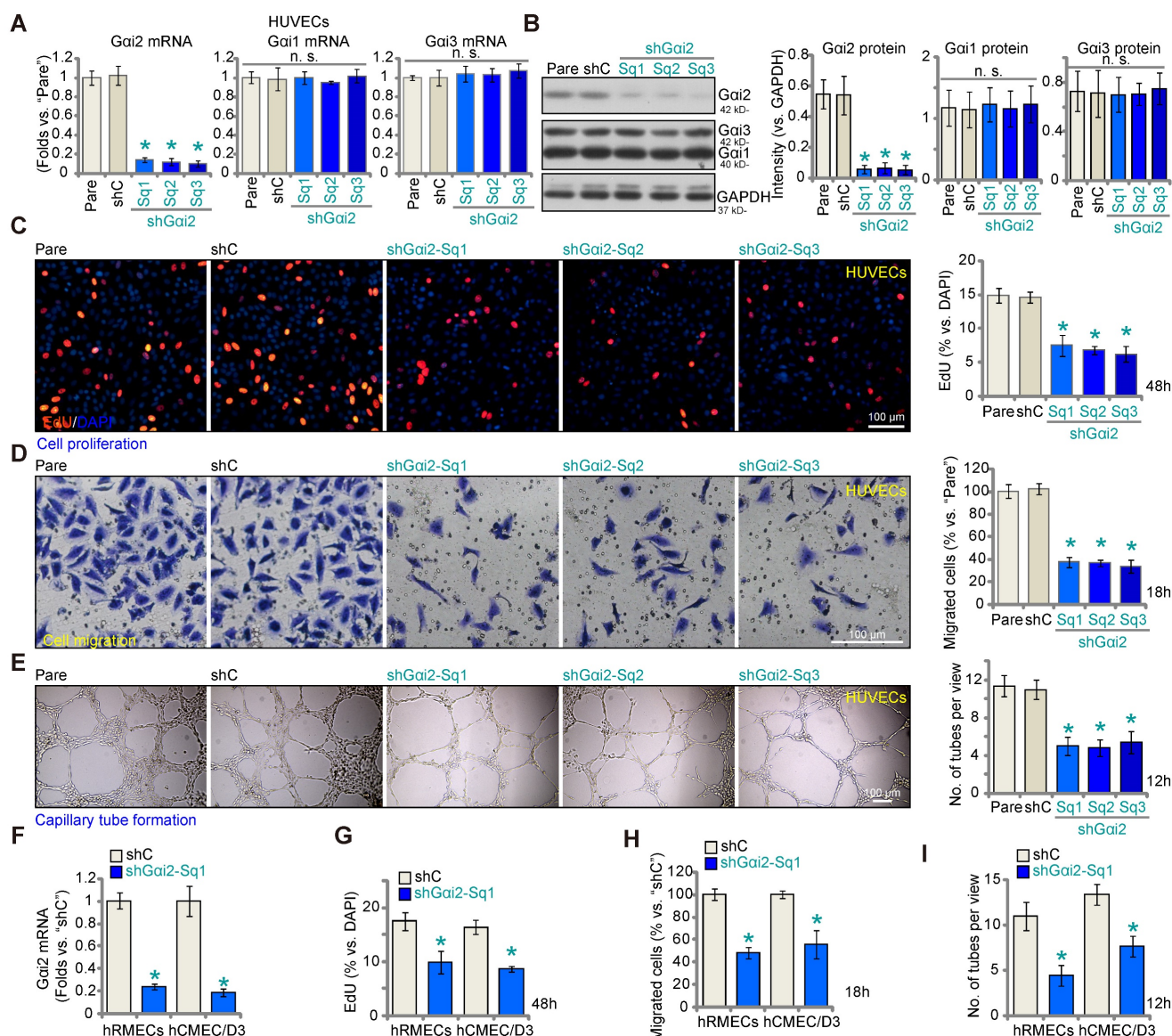


**Figure 2. Gai2 silencing impedes *in vitro* angiogenesis in cultured endothelial cells.** The mRNA (A) and protein (B) expression of Gai1/2/3 in stable human umbilical vein endothelial cells (HUVEC) with the listed Gai2 shRNA (shGai2-Sq1, shGai2-Sq2 or shGai2-Sq3), scramble shRNA ("shC") or in parental control ("Pare") HUVECs were shown; The exact same number of the above HUVECs were maintained under complete medium and cultivated for designated hours, *in vitro* cell proliferation (by measuring nuclear EdU incorporation, C), migration ("Transwell" assays, D) and capillary tube formation (E) were examined. Gai2 mRNA expression in human retinal microvascular endothelial cells (hRMECs) and human cerebral microvascular endothelial cells (hCMEC/D3) with shC or shGai2-Sq1 was shown (F); The endothelial cells were maintained under complete medium and cultivated for designated hours, *in vitro* cell proliferation (G), migration (H) and capillary tube formation (I) were tested similarly, with results quantified. Data were expressed as mean  $\pm$  standard deviation (SD). The quantifications were from five biological repeats (n = 5). \*P < 0.05 versus "shC" group. "n.s." stands for non-statistical differences (P > 0.05). Scale bar = 100  $\mu$ m.



HUVECs exhibited a remarkable increase in *Gai2* mRNA levels, exceeding 10- to 15-fold elevation (Figure 5A), while *Gai1* and *Gai3* mRNA levels remained unchanged (Figure 5A). Notably, *Gai2* protein upregulation was also observed in oe*Gai2*-Slc1 and oe*Gai2*-Slc2 HUVECs, with *Gai1* and *Gai3* protein expression remaining unaltered (Figure 5B). Ectopic over-expression of *Gai2* induced pro-angiogenic activity, as evidenced by a significant increase in cell proliferation (tested via the ratio of EdU-positive nuclei) in oe*Gai2*-Slc1 and oe*Gai2*-Slc2 HUVECs (Figure 5C). Furthermore, oe*Gai2* treatment

accelerated *in vitro* migration (Figure 5D) and promoted capillary tube formation (Figure 5E) in HUVECs.

In other endothelial cell types, hRMECs and hCMEC/D3, stable over-expression of *Gai2* using the same lentiviral construct, oe*Gai2*, similarly resulted in a substantial upregulation of *Gai2* mRNA (Figure 5F). With *Gai2* over-expression, endothelial cells exhibited increased cell proliferation (nuclear EdU incorporation, Figure 5G), accelerated cell migration (Figure 5H), and augmented capillary tube formation (Figure 5I).

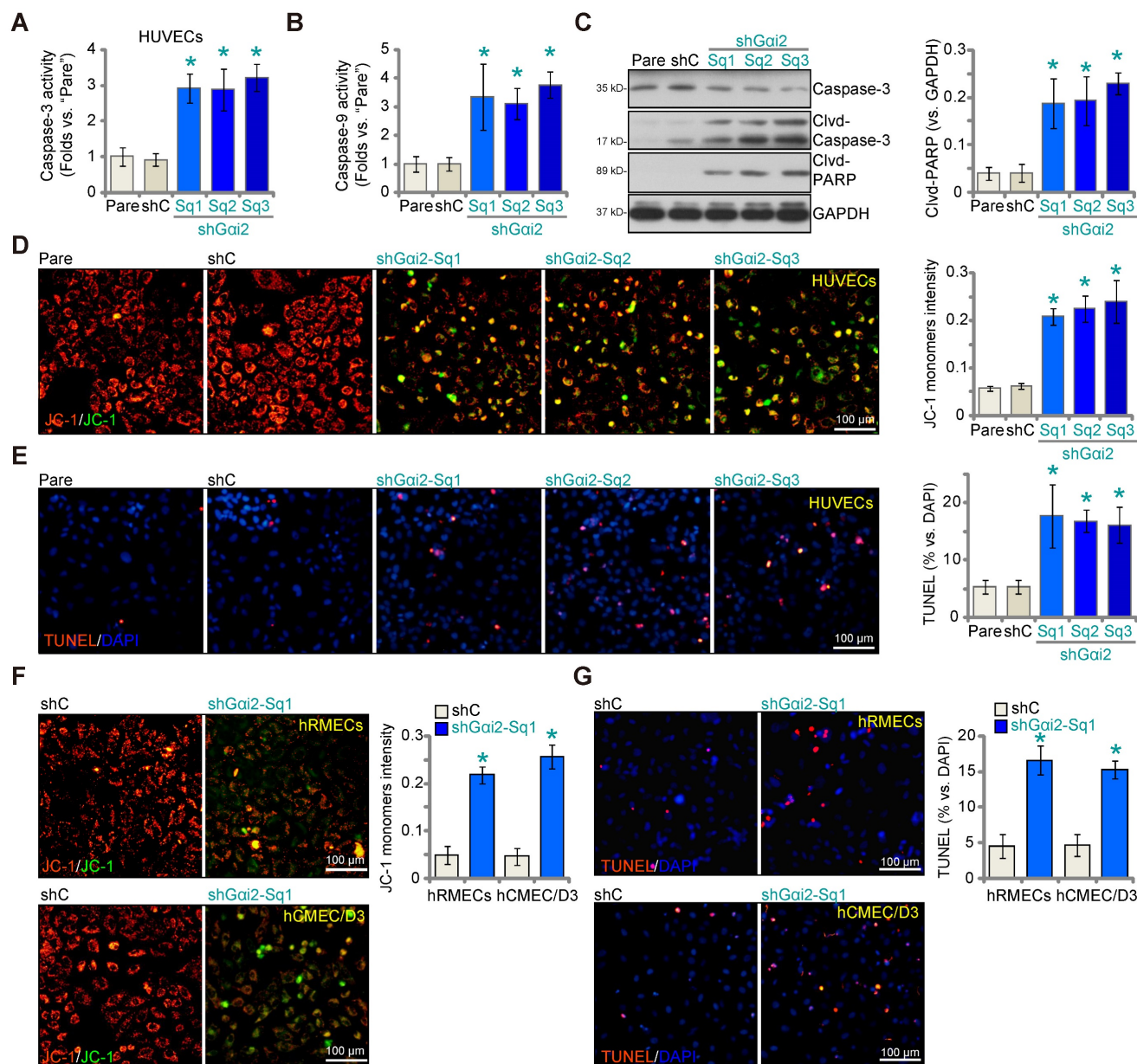


**Figure 3.** *Gai2* silencing provokes apoptosis in cultured endothelial cells. The exact same number of HUVECs with the listed *Gai2* shRNA (sh*Gai2*-Sq1, sh*Gai2*-Sq2 or sh*Gai2*-Sq3), scramble shRNA ("shC") or the parental control ("Pare") HUVECs were cultivated for 60h, Caspase-3/9-PARP activation/cleavages were tested (A-C); The depolarization of mitochondria was examined by quantifying aggregation of JC-1 green monomers (D); Cell apoptosis was tested by measuring TUNEL-positive nuclei ratio (E). The exact same number of hRMECs or hCMEC/D3 with shC or sh*Gai2*-Sq1 were cultivated for 60h, depolarization of mitochondria and apoptosis were respectively examined via JC-1 staining (F) and nuclear TUNEL staining assays (G). Data were expressed as mean  $\pm$  standard deviation (SD). Quantifications were from five biological repeats (n = 5). \* $P < 0.05$  versus "shC" group. Scale bar = 100  $\mu$ m.

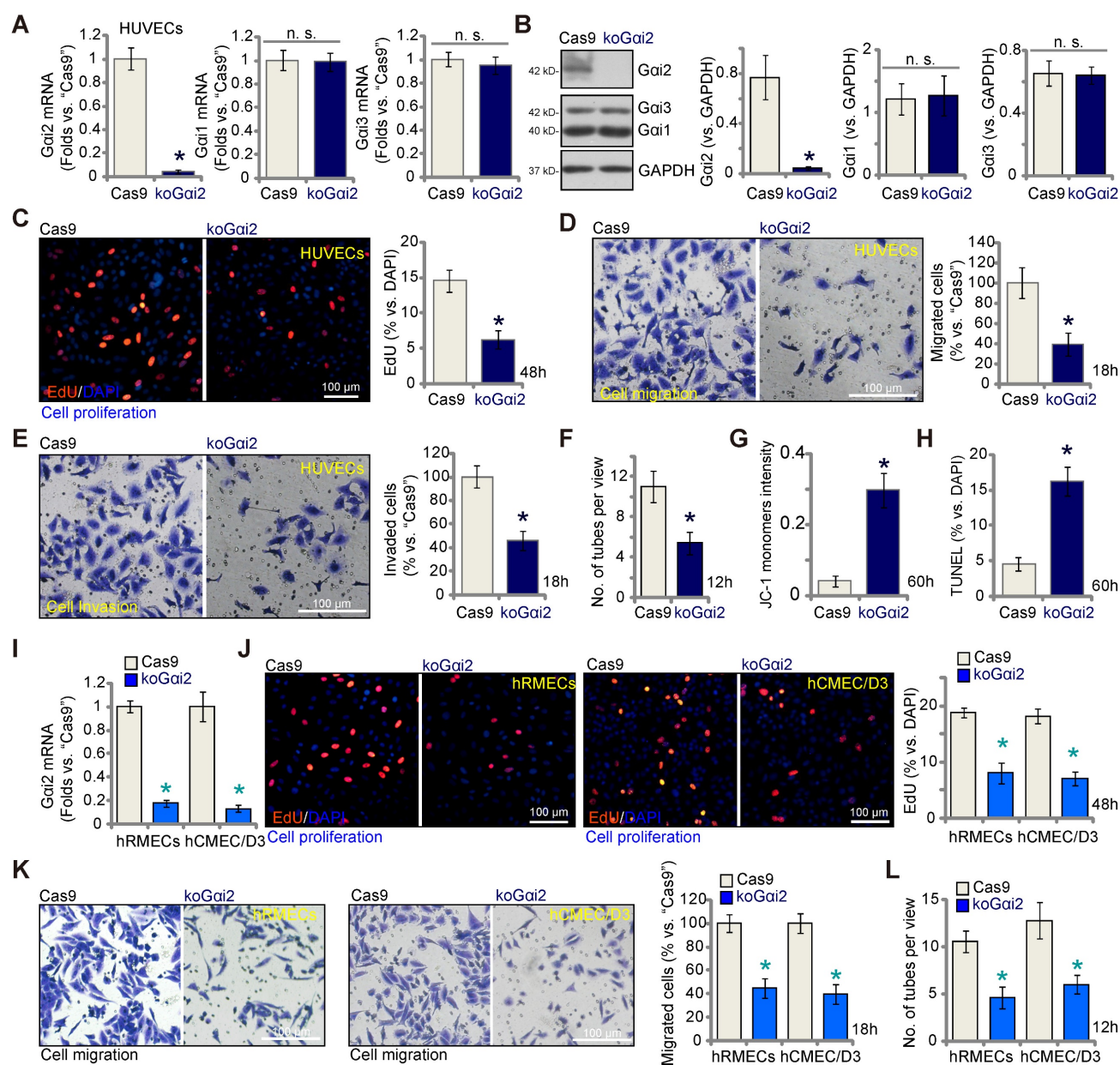


**Figure 4. Complete *Gai2* knockout (KO) leads to significant anti-angiogenic activity in cultured endothelial cells.** The mRNA (A) and protein (B) expression of *Gai1/2/3* in single stable HUVECs with both Cas9-expressing construct plus the CRISPR/Cas9-*Gai2*-KO construct ("koGai2") or the control construct ("Cas9") was shown. The exact same number of the above HUVECs were cultivated for designated hours, *in vitro* cell proliferation (by measuring nuclear EdU incorporation, C), migration ("Transwell" assays, D), invasion ("Matrigel Transwell" assays, E) and capillary tube formation (F) were tested; Depolarization of mitochondria and apoptosis were respectively examined via measuring JC-1 monomer intensity (G) and nuclear TUNEL ratio (H). *Gai2* mRNA expression in hRMECs or hCMEC/D3 with same CRISPR/Cas9 genetic treatment, "koGai2" or "Cas9", was shown (I); The exact same number of cells were cultivated for designated hours, *in vitro* cell proliferation (J), migration (K) and capillary tube formation (L) were tested similarly. Data were expressed as mean  $\pm$  standard deviation (SD). Quantifications were from five biological repeats ( $n = 5$ ). \* $P < 0.05$  versus "Cas9" group. "n.s." stands for non-statistical differences ( $P > 0.05$ ). Scale bar = 100  $\mu$ m.

## Gai2 is important for activation of the transcription factor NFAT in endothelial cells

A previous study demonstrated the significance of *Gai2* in triggering the activation of the transcription factor NFAT (nuclear factor of activated T cells) within skeletal muscle cells [38]. NFAT signaling plays a pivotal role in endothelial cell activation and angiogenesis [39, 40]. Therefore, we set out to study whether *Gai2* has an impact on NFAT activation in endothelial cells. As shown, *Gai2* silencing by

targeted shRNAs, sh*Gai2*-Sq1, sh*Gai2*-Sq2 and sh*Gai2*-Sq3, potentially decreased the NFAT-luciferase reporter activity in cultured HUVECs (Figure 6A). Expression of NFAT-dependent and pro-angiogenic genes, including *Egr3* (early growth response 3), *CXCR7* (C-X-C chemokine receptor 7) and *RND1* (Rho family GTPase 1) [40, 41], was also down-regulated by the shRNAs (Figure 6B). Ionomycin, known for its ability to activate the calcineurin-NFAT cascade [42], reinstated NFAT reporter activity in *Gai2*-silenced HUVECs (sh*Gai2*-Sq1) (Figure 6C). Additionally,



ionomycin significantly mitigated the inhibitory effects of Gai2 shRNA on HUVECs proliferation

(Figure 6D), migration (Figure 6E), and tube formation (Figure 6F).

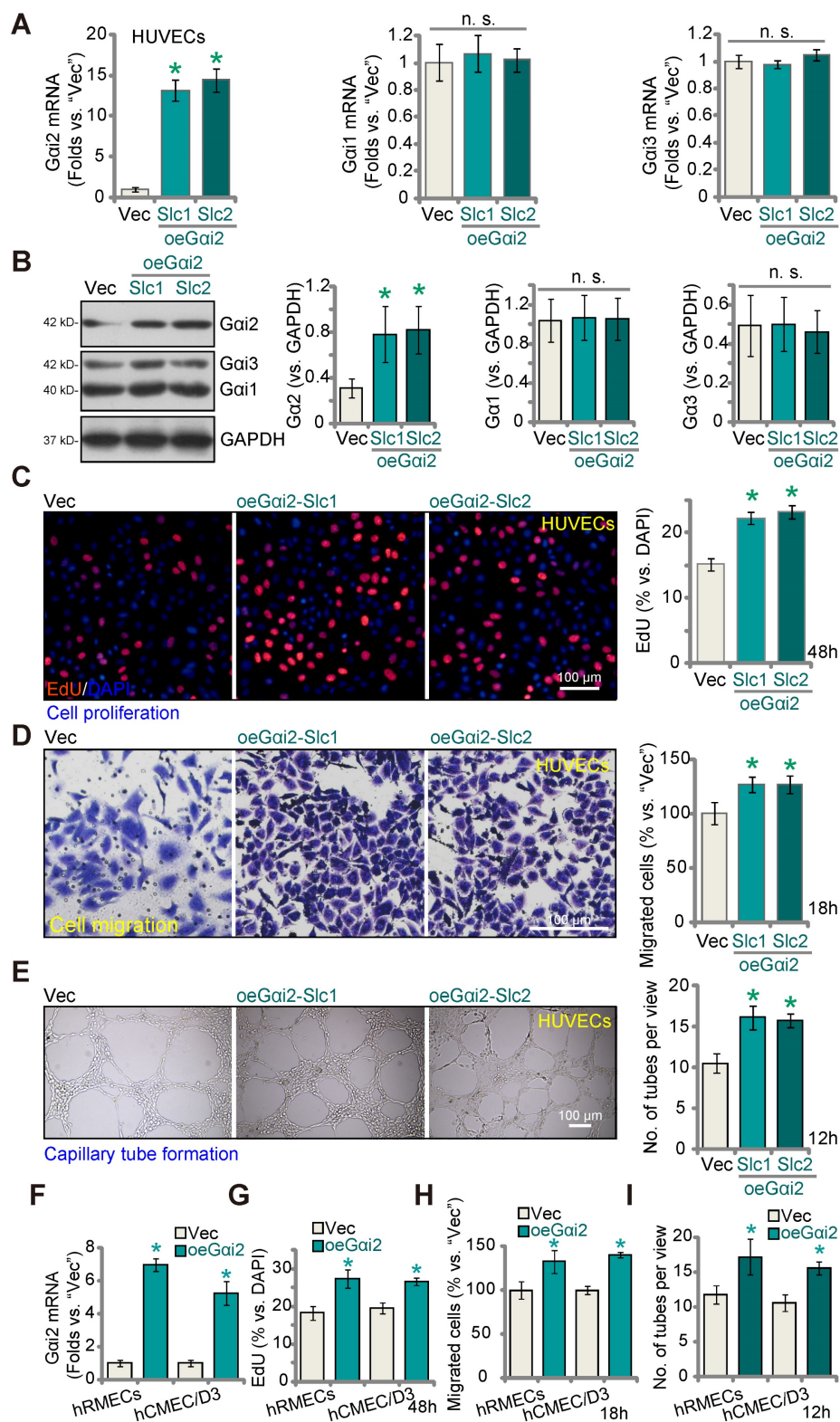


**Figure 5. Gai2 over-expression promotes angiogenesis in cultured endothelial cells.** The mRNA (A) and protein (B) expression of Gai1/2/3 in HUVECs with the Gai2-overexpressing construct (oeGai2-Slc1 and oeGai2-Slc2, representing two stable selections) or empty vector ("Vec") was shown; The exact same number of the above HUVECs were cultivated for designated hours, *in vitro* cell proliferation (by measuring nuclear EdU incorporation, C), migration ("Transwell" assays, D), and capillary tube formation (E) were tested. Gai2 mRNA expression in hRMECs or hCMEC/D3 with the Gai2-overexpressing construct (oeGai2) or empty vector ("Vec") was shown (F); The exact same number of cells were cultivated for designated hours, *in vitro* cell proliferation (G), cell migration (H) and capillary tube formation (I) were tested similarly. Data were expressed as mean  $\pm$  standard deviation (SD). Quantifications were from five biological repeats (n = 5). \*P < 0.05 versus "Vec" group. "n.s." stands for non-statistical differences (P > 0.05). Scale bar = 100  $\mu$ m.



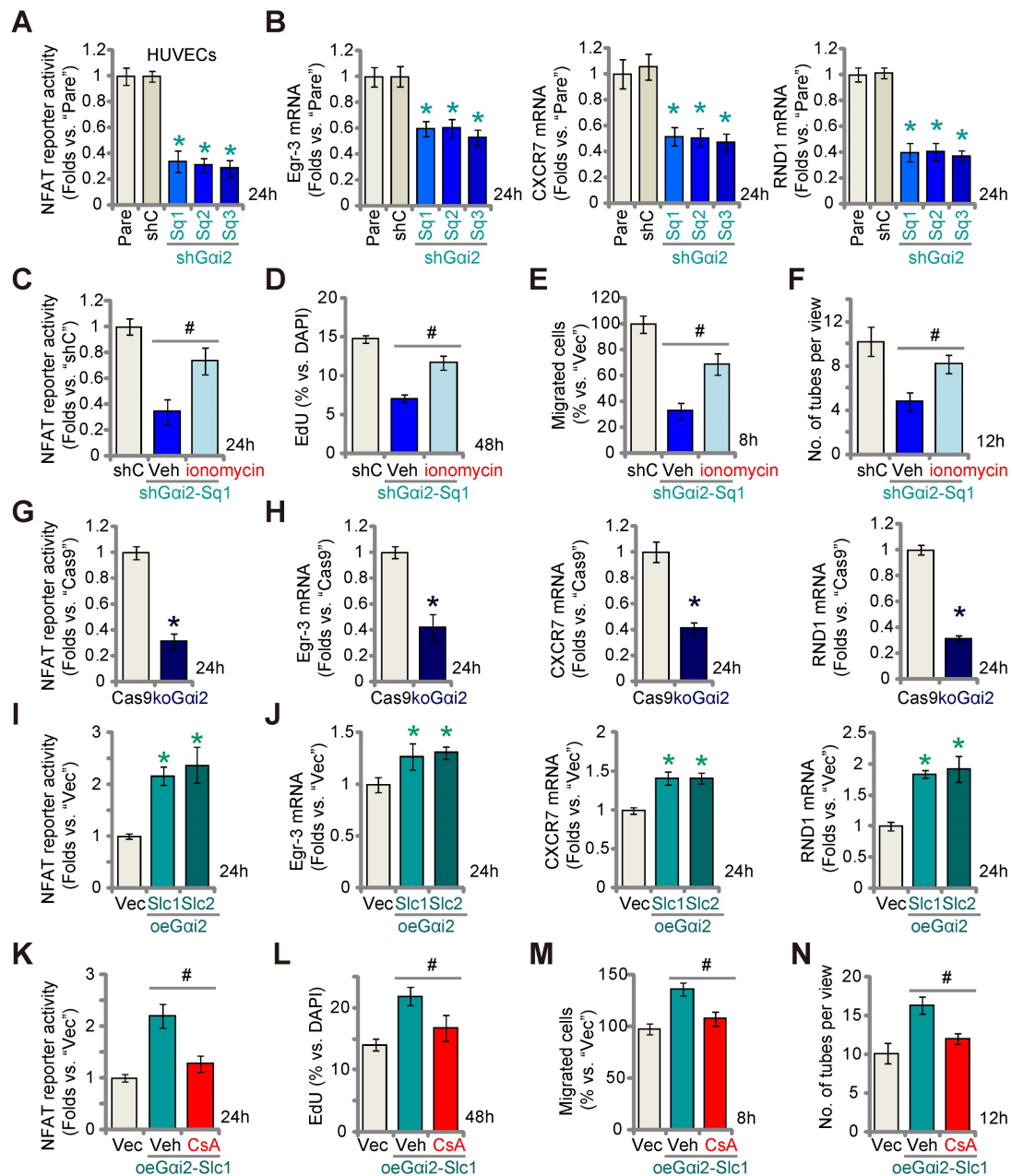


**Figure 6.** *Gai2* is important for activation of the transcription factor NFAT in endothelial cells. Stable HUVECs with the listed *Gai2* shRNA (shGai2-Sq1, shGai2-Sq2 or shGai2-Sq3), scramble nonsense shRNA ("shC"), Cas9-expressing construct plus the CRISPR/Cas9-*Gai2*-KO construct ("koGai2"), the control construct ("Cas9"), the *Gai2*-overexpressing construct (oeGai2-Slc1 and oeGai2-Slc2), empty vector ("Vec") were established, the NFAT-luciferase reporter activity was tested (**A**, **G** and **I**), and expression of listed mRNAs tested as well (**B**, **H** and **J**). Stable shGai2-Sq1-expressing HUVECs were treated with ionomycin (5  $\mu$ M) or vehicle control (DMSO) for listed hours, the NFAT-luciferase reporter activity was tested (**C**); The *in vitro* cell proliferation (by measuring nuclear EdU incorporation, **D**), migration ("Transwell" assays, **E**) and capillary tube formation (**F**) were measured, with results quantified. Stable shGai2-Sq1-expressing HUVECs were treated with cyclosporin A (CsA, 2.5  $\mu$ M) or vehicle control (DMSO) for listed hours, the NFAT-luciferase reporter activity was tested (**K**); The *in vitro* cell proliferation (**L**), cell migration (**M**) and capillary tube formation (**N**) were tested similarly, with results quantified. "Pare" stands for the parental control cells. Data were expressed as mean  $\pm$  standard deviation (SD). Quantifications were from five biological repeats (n = 5). \**P* < 0.05 versus "shC"/"Cas9"/"Vec" control cells (**A**, **B**, **G**, **J**). # *P* < 0.05 versus "Veh" treatment (**C**, **F**, **K**, **N**).

Similarly, CRISPR/Cas9 KO of *Gai2* largely decreased NFAT-luciferase reporter activity (Figure 6G) and down-regulated *Egr3*, *CXCR7* and *RND1* (Figure 6H) in cultured HUVECs. In contrast, in the *Gai2*-overexpressing HUVECs, oeGai2-Slc1 and oeGai2-Slc2, NFAT-luciferase reporter activity was strengthened (Figure 6I) and expression of NFAT-dependent genes was up-regulated (Figure 6J). CsA, an established NFAT inhibitor [43, 44], blocked

the increased NFAT reporter activity observed in oeGai2-Slc1 HUVECs (Figure 6K). Functionally, the *Gai2* over-expression-induced enhancement in HUVECs proliferation (Figure 6L), migration (Figure 6M), and capillary tube formation (Figure 6N) were reversed by CsA. These results further support that *Gai2* promotes endothelial cell activation through the upregulation of NFAT signaling.

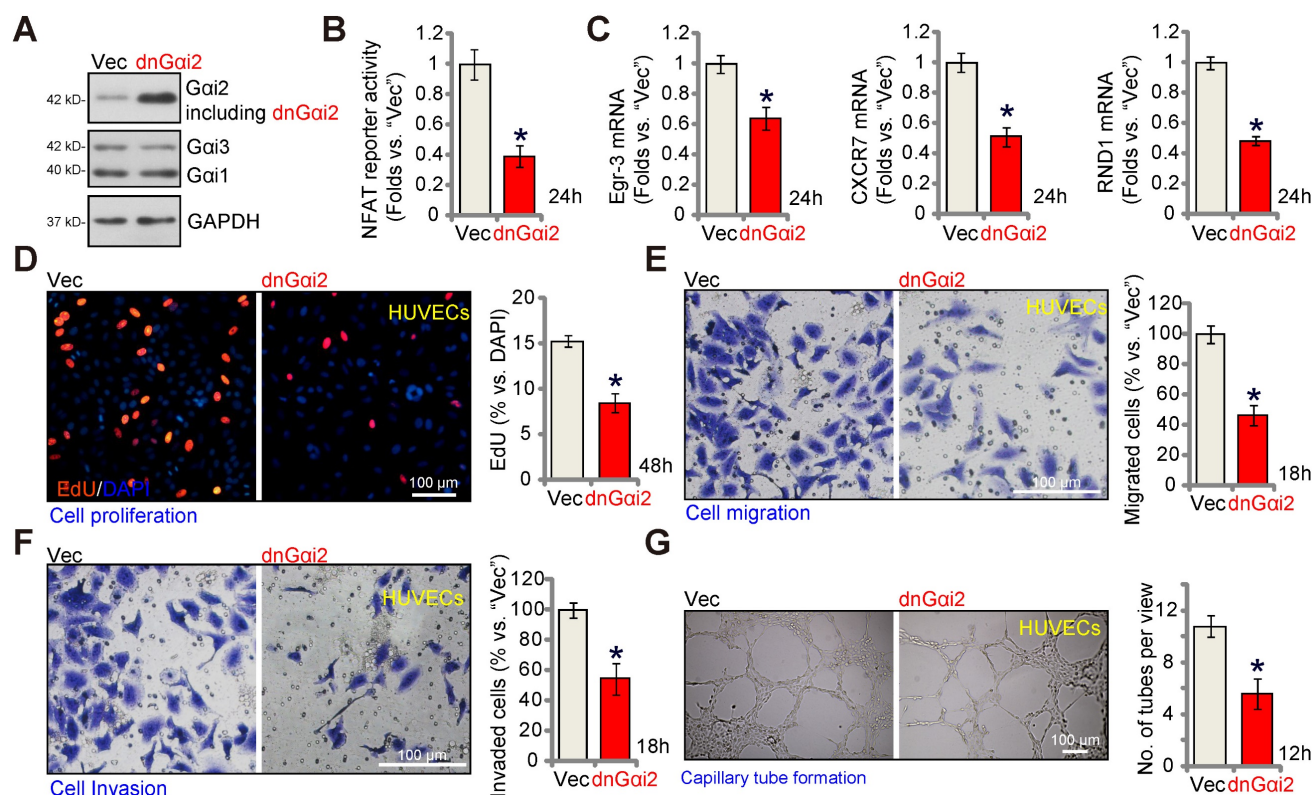


**Figure 7. A dominant negative Gai2 hinders *in vitro* angiogenesis in cultured endothelial cells.** The expression of Gai1/2/3 in stable HUVECs with the dominant negative mutant Gai2 (S48C, "dnGai2") or the empty vector ("Vec") was shown (A); The NFAT-luciferase reporter activity (B) and expression of listed mRNAs (C) were measured as well. The exact same number of the above HUVECs were cultivated for designated hours, *in vitro* cell proliferation (by measuring nuclear EdU incorporation, D), migration ("Transwell" assays, E), invasion ("Matrigel Transwell" assays, F) and capillary tube formation (G) were also tested, with results quantified. Data were expressed as mean  $\pm$  standard deviation (SD). Quantifications were from five biological repeats ( $n = 5$ ). \* $P < 0.05$  versus "Vec" control cells.

## A dominant negative Gai2 hinders *in vitro* angiogenesis in cultured endothelial cells

The key step for the activation of heterotrimeric G proteins involves the GTP binding process, causing the separation of subunits and producing GTP-bound  $\alpha$  subunits alongside liberated  $\beta\gamma$  complexes. A dominant negative mutation, Gai2 (S48C), is known to completely disrupt GTP binding and inhibit Gai2 activation [28, 45]. A lentiviral dominant negative Gai2 (dnGai2) construct was stably transduced into HUVECs, and stable cells formed after puromycin selection. Western blot assay results, Figure 7A, confirmed expression of dnGai2 alongside the wild type Gai2 in the stable HUVECs, and Gai1 and Gai3 expression remained unchanged (Figure 7A). Importantly, dnGai2 decreased NFAT-luciferase reporter activity (Figure 7B) and down-regulated NFAT-dependent gene expression (*Egr3*, *CXCR7* and *RND1*) (Figure 7C). The dnGai2 also induced anti-angiogenic activity HUVECs, inhibiting proliferation (EdU ratio reduction, Figure 7D), *in vitro* cell migration (Figure 7E) and invasion (Figure 7F). Moreover, capillary tube formation was also inhibited in dnGai2-expressing HUVECs (Figure 7G).

## Endothelial knockdown of Gai2 inhibits retinal angiogenesis in mice

To explore the potential influence of Gai2 on *in vivo* angiogenesis, we carried out experiments using the mouse retinal vasculature, as previously described [46]. Initially, adult mice underwent intravitreal injection of murine AAV5-TIE1-Gai2 shRNA (no Taq), which was driven by the endothelial cell-specific TIE1 promoter [9, 12]. This intervention effectively reduced Gai2 expression exclusively in endothelial cells, referred to as "Gai2-eKD". As a genetic control treatment, murine AAV5-TIE1-scramble control shRNA ("aav-shC") [46] was administered to the mouse retina. Three weeks after the virus injection, we collected murine retinal tissues and analyzed tissue lysates. In Gai2-eKD mice, *Gai2* mRNA (Figure 8A) and protein (Figure 8B) levels were significantly decreased, while Gai1 and Gai3 mRNA (Figure 8A) and protein (Figure 8B) levels remained unchanged. Additionally, endothelial knockdown of Gai2 led to a reduction in the expression of NFAT-dependent genes (*Egr3*, *CXCR7* and *RND1*) in the retinal tissues (Figure 8C).

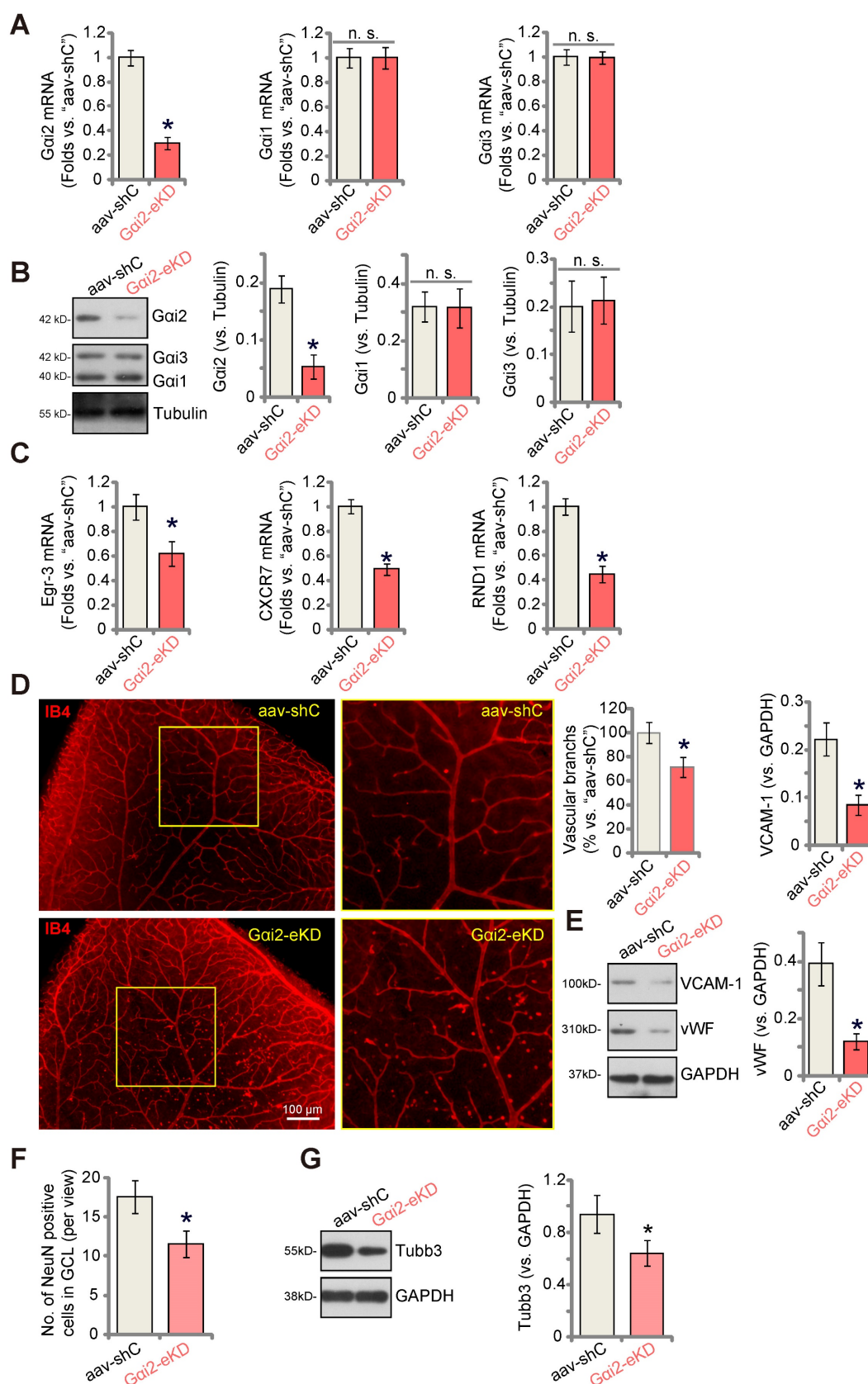


**Figure 8. Endothelial knockdown of *Gai2* inhibits retinal angiogenesis in mice.** Adult C57BL/6 mice ( $32.40 \pm 2.32$ -day old, three male two female in each group) received intravitreal injections of either murine AAV5-TIE1-*Gai2* shRNA ("Gai2-eKD", 0.1  $\mu$ L) or AAV5-TIE1 scramble control shRNA ("aav-shC", 0.1  $\mu$ L). After a twenty-one-day period, expression of listed mRNAs and proteins in murine retinal tissues was tested (**A–C**, **E** and **G**). Additionally, the retinal vasculature was visualized using retinal isolectin B4 (IB4) staining (**D**). In the retinal slides, NeuN/DAPI immunofluorescence staining was performed, and the quantification of NeuN-positive RGCs within GCL was conducted (**F**). "GCL": ganglion cell layer, "ONL": Outer nuclear layer, "INL": Inner nuclear layer. Data were expressed as mean  $\pm$  standard deviation (SD). Quantifications were from five biological repeats ( $n = 5$ ). \* $P < 0.05$  versus "aav-shC" group. Scale bar = 50/100  $\mu$ m.



Examination of retinal vasculature through IB4 staining demonstrated a strong inhibition of angiogenesis in the mouse retina following endothelial knockdown of *Gai2* (Figure 8D). *Gai2*-eKD mice displayed a marked decrease in the number of retinal vascular branches and branch points (Figure 8D). Furthermore, the endothelial marker proteins, von Willebrand factor (vWF) and VCAM-1, exhibited reduced expression in retinal tissues following *Gai2*-eKD (Figure 8E). Therefore, endothelial knockdown of *Gai2* effectively suppressed retinal angiogenesis in mice.

When retinal angiogenesis is disrupted, retinal ganglion cells (RGCs), the neuronal cells within the retina, become highly susceptible to cell death due to the deprivation of oxygen, energy, and essential nutrients [9, 12]. This constitutes a fundamental pathology in various retinal disorders, including diabetic retinopathy (DR), retinopathy of prematurity (ROP), and neovascular glaucoma [47]. We thus conducted an analysis to test whether the endothelial knockdown of *Gai2* had an impact on RGCs within the mouse retina. Quantification of retinal immunofluorescence images revealed a reduction in the number of NeuN-positive RGCs within the ganglion cell layer (GCL) following endothelial *Gai2* knockdown (Figure 8F). *Tubb3* (beta-III tubulin) is a marker for the structural integrity and health of RGCs in the retina. We showed that the expression of *Tubb3* protein was down-regulated in the retinal tissues of *Gai2*-eKD mice (Figure 8G), further supporting RGC degeneration.

### Endothelial over-expression of *Gai2* strengthens retinal angiogenesis in mice

To further substantiate the role of *Gai2* in angiogenesis *in vivo*, we performed an intravitreal injection of a murine AAV5-TIE1-*Gai2*-expressing construct, referred to as "*Gai2*-eOE", in adult mice to induce over-expression of *Gai2* in endothelial cells. Control mice received intravitreal injection of AAV5-TIE1-Vec ("*aav*-Vec"). Following the injections, we collected and analyzed retinal tissues. Our findings revealed a significant increase in *Gai2* mRNA (Figure 9A) and protein (Figure 9B) expression in the retinal tissues of *Gai2*-eOE mice. The expression of *Gai1* and *Gai3* remained unchanged (Figure 9A and B). Furthermore, the expression of NFAT-dependent genes, specifically *Egr3*, *CXCR7*, and *RND1*, exhibited an upregulation in the retinal tissues of *Gai2*-eOE mice (Figure 9C), suggesting the activation of NFAT signaling. Visual examination of retinal vasculature through IB4 staining confirmed a significant increase in angiogenesis in the mouse retina following

endothelial over-expression of *Gai2* (Figure 9D). *Gai2*-eOE mice displayed a marked increase in the number of retinal vascular branches and branch points (Figure 9D). Additionally, vWF and VCAM-1 protein expression was also elevated (Figure 9E). These findings collectively support that endothelial over-expression of *Gai2* enhances retinal angiogenesis in mice.

### Endothelial *Gai2* silencing ameliorates retinal pathological angiogenesis in diabetic retinopathy mice

Pathological angiogenesis is a key pathology of diabetic retinopathy (DR) [48-53]. We next explored the potential role of *Gai2* in the process. We first utilized publicly available single-cell RNA sequencing data (GEO: #GSE209872) obtained from STZ-induced diabetic mice to delineate the cellular localization of *Gai2* within the diabetic retina. Employing reduction in dimensions, clustering techniques, and annotation, the individual cells across the retina were segregated into 12 distinct clusters, which were subsequently visualized using UMAP projections (Figure 10A). Next, through specifically focusing on *Gai2* expression, our analysis revealed a significant presence of *Gai2* within endothelial cells (Figure 10B and C). This observation underscores the specific localization of *Gai2* in endothelial cells within the diabetic retina in mice.

Next, we assessed *Gai2* expression in mice subjected to streptozotocin (STZ) injections. Retinal tissues from both STZ-injected diabetic retinopathy (DR) mice and control mice were collected 90 days post the final STZ injection. In the DR mouse retinal tissues, there was a significant increase in *Gai2* mRNA expression (Figure 10D). Additionally, *Gai2* protein upregulation was observed in retinal tissues of two representative DR mice (Figure 10E). Combining data from all eight sets of blots revealed a significant upregulation of *Gai2* protein in retinal tissues of STZ-induced DR mice (Figure 10F).

To investigate the potential involvement of increased *Gai2* expression in the abnormal retinal angiogenesis observed in DR mice, an intravitreal injection of AAV5-TIE1-*Gai2* shRNA was administered into the retinas of DR mice ("*Gai2*-eKD") 30 days after the last STZ treatment. Control DR mice received an intravitreal injection of AAV5-TIE1 scramble control shRNA ("*aav*-shC"). After an additional 60 days, fresh retinal tissues were collected and analyzed. Results demonstrated a reduction in both *Gai2* mRNA and protein expression in the retinal tissues of *Gai2*-eKD DR mice (Figure 10G and H).

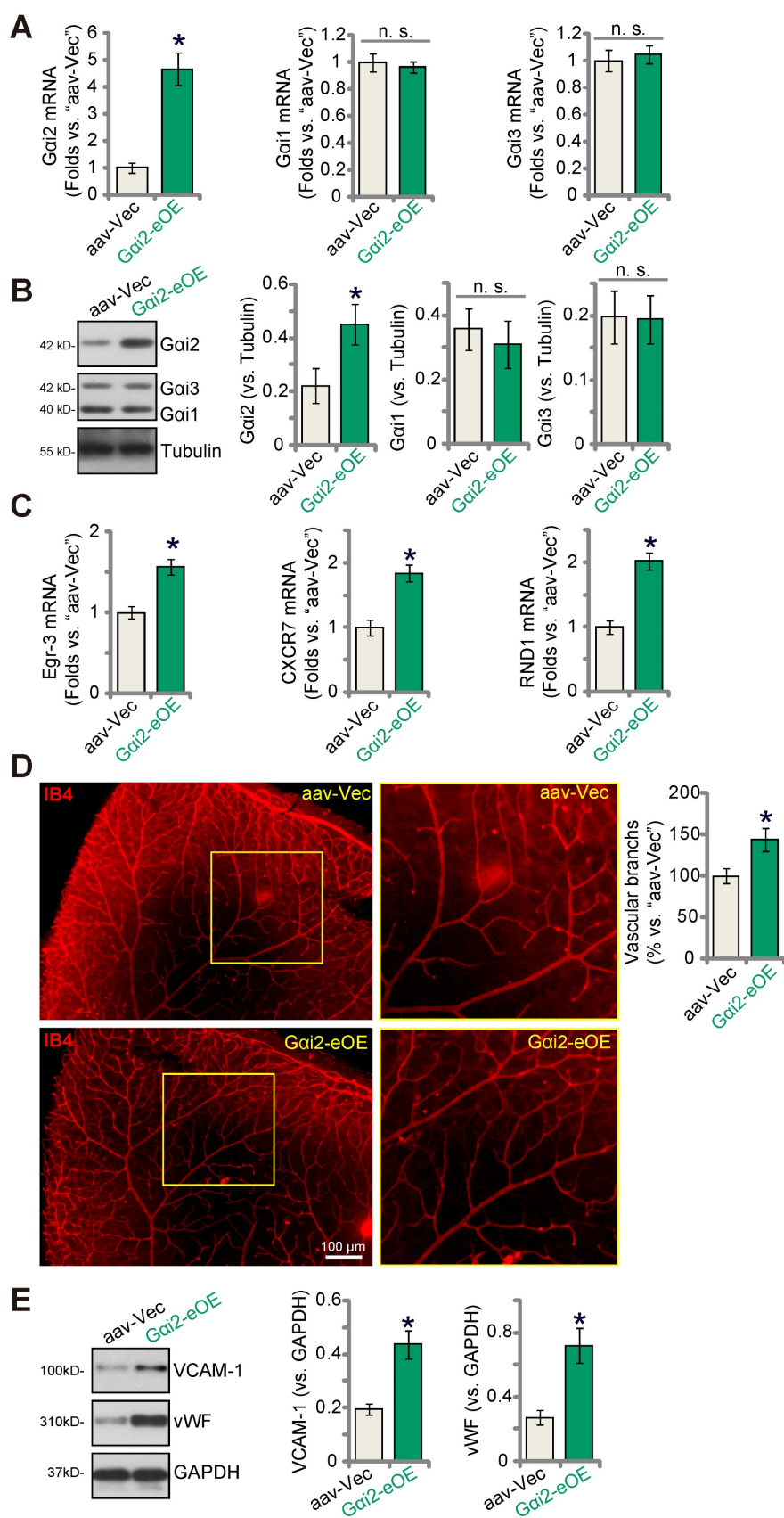


**Figure 9. Endothelial over-expression of *Gai2* strengthens retinal angiogenesis in mice.** Adult C57BL/6 mice ( $31.30 \pm 2.45$  day old, three male two female in each group) received intravitreal injections of either murine AAV5-TIE1-*Gai2*-expressing construct ("*Gai2*-eOE", 0.1  $\mu$ L) or AAV5-TIE1-vector ("aav-Vec", 0.1  $\mu$ L). After a twenty-one-day period, expression of listed mRNAs and proteins in murine retinal tissues was tested (**A-C**, and **E**). Additionally, the retinal vasculature was visualized using retinal isolectin B4 (IB4) staining (**D**). Data were expressed as mean  $\pm$  standard deviation (SD). Quantifications were from five biological repeats ( $n = 5$ ). \* $P < 0.05$  versus "aav-Vec" group. Scale bar = 100  $\mu$ m.

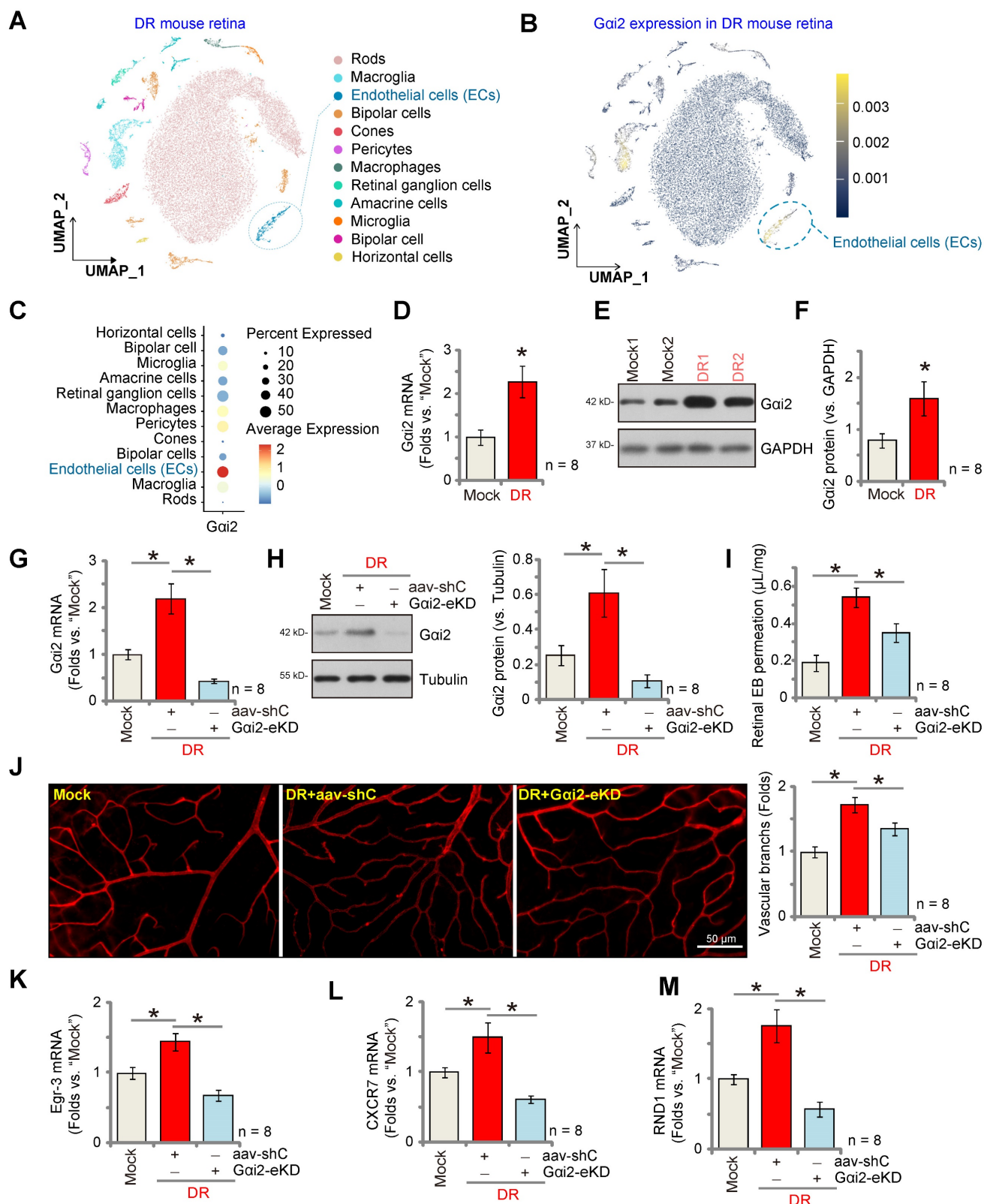


**Figure 10. Endothelial *Gai2* silencing ameliorates retinal pathological angiogenesis in diabetic retinopathy mice.** The publicly accessible scRNA-seq data (GEO: #GSE209872) obtained from STZ-induced diabetic mice through Uniform Manifold Approximation and Projection (UMAP) projections were displayed (A). The density plot reveals the expression and spatial distribution of *Gai2* in retinas, with the expression density scale depicted on the right side of the plot (B). Analysis based on single-cell data demonstrates the expression profiles of *Gai2* across different retinal cell types in STZ mice (C). Ninety days post the final STZ administration, retinal tissues from diabetic retinopathy ("DR") and "Mock" control mice (31.94 ± 1.98 day old, half male half female) were collected for the analysis of *Gai2* mRNA and protein expression (D-F). Thirty days after the last STZ treatment, mice received intravitreal injections of murine AAV5-TIE1-*Gai2* shRNA ("*Gai2*-eKD", 0.1 μL) or AAV5-containing scramble control shRNA ("aav-shC", 0.1 μL). After an additional 60 days, examination of listed mRNA and protein expression in retinal tissues was conducted (G, H, K-M). Alternatively, mice underwent Evans blue (EB) infusion for 2h, and the subsequent EB leakage was quantified (I). IB4 staining was conducted to visualize the retinal vasculature (J, scale bar = 50 μm). "Mock" refers to mice administered with citrate buffer. Each group consisted of eight mice (n = 8). \*P < 0.05 compared to "Mock" (D-F). \*P < 0.05 (G-M).



When compared to the Mock control mice, there was an increase in retinal vascular leakage measured by Evans blue (EB) staining in AAV-shC DR mice (Figure 10I). Furthermore, IB4 staining revealed increased vascular complexity (angiogenesis) in the retinas of DR mice (Figure 10J). Significantly, *Gai2*-eKD markedly suppressed the pathological retinal angiogenesis in DR mice (Figure 10I and J), reducing vascular leakage (Figure 10I) and diminishing vascular complexity (Figure 10J). Additionally, within the retinal tissue of aav-shC DR mice, there was a significant increase in the expression of NFAT-dependent genes (*Egr3*, *CXCR7*, and *RND1*) (Figure 10K-M), which was abolished following *Gai2*-eKD treatment (Figure 10K-M). Collectively, these results provide support that increased expression of *Gai2* played a significant role in the pathological retinal angiogenesis observed in DR mice.

## Discussion

Our recent research underscores the crucial roles of *Gai1* and *Gai3*, two other members of *Gai* protein family, in angiogenesis [9-13]. These proteins are essential for angiogenesis induced by stem cell factor (SCF) via interacting with the SCF-activated receptor c-Kit, initiating Akt-mTOR cascade activation in endothelial cells [10]. Silencing, KO (via CRISPR/Cas9), or introducing dominant negative mutations for *Gai1* and *Gai3* significantly impeded SCF-induced Akt-mTOR activation and angiogenesis [10]. *Gai1* and *Gai3* also form a complex with Netrin-1-stimulated receptor CD146, promoting angiogenesis *in vitro* and *in vivo* through downstream Akt-mTOR activation [11]. Moreover, phosphoenolpyruvate carboxykinase 1 (PCK1) regulates *Gai3* expression and downstream Akt-mTOR activation by enhancing the transcription activity of GATA binding protein 4 (GATA4) [12]. Our research also shows the essential roles of *Gai1* and *Gai3* in mediating vascular endothelial growth factor (VEGF)-induced VEGFR2 endocytosis, leading to downstream Akt-mTOR and Erk-MAPK activation, thereby promoting angiogenesis [13]. In addition, our findings emphasize the importance of *Gai1* and *Gai3*'s interaction with the RSPO3 (R-spondin 3)-activated receptor leucine-rich repeat G protein-coupled receptor 4 (LGR4) for downstream Akt-mTOR activation and angiogenesis [9].

In the present study, we demonstrate the pivotal role of *Gai2* in the activation of endothelial cells and the promotion of angiogenesis. Analysis of single-cell RNA sequencing data revealed increased *Gai2* expression in endothelial cells of OIR mice. Moreover, transcriptome analysis linking *Gai2* to angiogenesis-

related processes/pathways, supported by increased *Gai2* expression in experimental OIR mouse retinal tissues, highlights its role in angiogenesis.

Using various endothelial cell types, including HUVECs, hRMECs, and hCMEC/D3, we employed targeted shRNA silencing and CRISPR/Cas9 KO techniques to suppress *Gai2* expression. *Gai2* deficiency led to a robust reduction in cell proliferation, migration, invasion, and capillary tube formation. Additionally, a notable increase in apoptosis was observed in *Gai2*-silenced or -KO endothelial cells. Conversely, ectopic over-expression of *Gai2* displayed pro-angiogenic effects in cultured endothelial cells, enhancing cell proliferation, migration, invasion, and capillary tube formation. Contrarily, the introduction of a dominant negative mutation in *Gai2* effectively inhibited endothelial cell activation. *In vivo* experiments using endothelial-specific *Gai2* shRNA AAV inhibited retinal angiogenesis in mouse retinal tissues. Conversely, endothelial *Gai2* over-expression strengthened retinal angiogenesis in mice. Thus, *Gai2* is essential for endothelial cell activation and angiogenesis.

NFAT is a family of transcription factors central to the regulation of gene expression in immune cells, particularly T lymphocytes [54-56]. Upon activation, NFAT is translocated from the cytoplasm to the nucleus, where it orchestrates the transcription of various genes (such as various cytokines) [54-56]. NFAT activation is tightly controlled, primarily through signaling pathways including the calcium-calcineurin pathway [54-56]. NFAT transcription factors exist in multiple isoforms and are not limited to T cells, as they play roles in B cell activation, mast cell degranulation, neuronal plasticity, carcinogenesis, muscle development and other processes [54-58].

NFAT plays a significant role in endothelial cell activation and angiogenesis. When endothelial cells are exposed to specific stimuli, NFAT promotes the expression of genes essential for endothelial cell activation [39-41, 59]. Suehiro *et al.*, have shown that VEGF activates the NFAT cascade in endothelial cells and induces NFATc1 binding of its targeted genes, including *CXCR7* and *RND1*, thereby promoting their expression [40]. VEGF activates NFAT and increases its binding with the target gene *Egr-3*, thereby promoting expression of *Egr-3* [41]. The latter is required for endothelial cell proliferation, migration, and tube formation [41]. Armesilla *et al.*, also showed that VEGF induced NFAT dephosphorylation and nuclear translation, thereby increasing tissue factor (TF) promoter activity and expression [59]. CsA, an established NFAT inhibitor, or dominant negative mutation of NFAT inhibits VEGF-induced TF promoter activation in HUVECs [59]. Hernández and

colleagues reported that NFAT inhibition by CsA suppresses VEGF-induced endothelial cell activation and hinders angiogenesis [39].

In skeletal muscle cells *Gai2* triggers phospholipase C (PLC) activation, leading to the production of inositol trisphosphate (IP<sub>3</sub>) and subsequent release of intracellular calcium (Ca<sup>2+</sup>) [38]. The latter then activates calcineurin, a phosphatase that dephosphorylates NFAT proteins [38]. Dephosphorylated NFAT then translocates from the cytoplasm to the nucleus, where it modulates targeted gene expression [38]. Our results indicate that *Gai2*-driven endothelial cell activation and angiogenesis are primarily mediated by promoting NFAT activation. In HUVECs, *Gai2* silencing, KO or dominant negative mutation results in decreased NFAT-luciferase reporter activity and down-regulation of NFAT targets (*Egr3*, *CXCR7*, and *RND1*), whereas *Gai2* over-expression leads to their upregulation. Notably, the calcineurin-NFAT activator ionomycin rescues NFAT activity, significantly mitigating the inhibitory effects of *Gai2* shRNA on HUVECs proliferation, migration, and tube formation. Conversely, the enhancement in HUVECs proliferation, migration and tube formation induced by *Gai2* over-expression were reversed by the NFAT inhibitor CsA. *In vivo*, down-regulation of NFAT target genes (*Egr3*, *CXCR7*, and *RND1*) in mouse retinal tissues with endothelial knockdown of *Gai2* was detected. Whereas NFAT-dependent genes were up-regulated in mouse retinal tissues with endothelial *Gai2* over-expression. NFAT-dependent genes were also up-regulated in retinal tissues of DR mice. Therefore, *Gai2*-mediated endothelial cell activation and angiogenesis are associated with NFAT activation.

DR is a complex condition characterized by two main stages: non-proliferative diabetic retinopathy (NPDR) and proliferative diabetic retinopathy (PDR) [48-50, 60]. The transition from NPDR to PDR marks the appearance of abnormal, delicate blood vessels in the retina, prone to leakage and causing issues like retinal edema, hemorrhage, fibrovascular growth, and retinal detachment [48-50, 60-62]. This pathological angiogenesis primarily arises from damage to blood vessels due to long-term high blood sugar levels, exacerbated by inflammatory and oxidative stress factors [48-50, 60-62]. The interaction between these harmful elements triggers the increase of key agents promoting blood vessel growth, including VEGF, leading to the formation of abnormal blood vessels in the oxygen-deprived retinal environment [52, 53, 60, 63].

Here, examination of single-cell RNA sequencing data and experiments demonstrated significantly increased levels of *Gai2* specifically in retinal

endothelial cells of mice with STZ-induced DR. Importantly, targeted silencing of *Gai2* in retinal endothelial cells, achieved through intravitreal administration of AAV5-TIE1-*Gai2* shRNA, effectively mitigated pathological retinal angiogenesis in the DR murine models. Based on these findings, we propose that increased *Gai2* over-expression plays a pivotal role in pathological angiogenesis in DR, emerging as a promising and relevant therapeutic target.

## Supplementary Material

Supplementary figure.

<https://www.thno.org/v14p2190s1.pdf>

## Acknowledgements

### Funding

This work was generously supported by grants from the National Natural Science Foundation of China (82371473, 82171461, 81771457, 82172425 and 81922025); A Project Funded by the Priority Academic Program Development of Jiangsu Higher Education Institutions; Jiangsu Provincial Medical Key Discipline (Laboratory) Cultivation Unit (JSDW202223), the Social Development Key Programs of Jiangsu Province-Advanced Clinical Technology (BE2023705).

### Ethics

This study was approved by the Ethics Committee of Soochow University.

### Author contribution statement

CB, YN, XZ KL CL, and CC conceived, designed, and supervised the study. CB, YN, KL, JZ, JY CL, and CC analyzed the data. All listed authors performed the experiments and the statistical analysis, and wrote the manuscript and revise it. All authors read the manuscript and approved the final version.

### Data availability statement

The data are included in the article.

### Competing Interests

The authors have declared that no competing interest exists.

## References

1. Dudley AC, Griffioen AW. Pathological angiogenesis: mechanisms and therapeutic strategies. *Angiogenesis*. 2023; 26: 313-47.
2. Risau W, Flamme I. Vasculogenesis. *Annu Rev Cell Dev Biol*. 1995; 11: 73-91.
3. Eelen G, Treps L, Li X, Carmeliet P. Basic and Therapeutic Aspects of Angiogenesis Updated. *Circ Res*. 2020; 127: 310-29.
4. Betz C, Lenard A, Belting HG, Affolter M. Cell behaviors and dynamics during angiogenesis. *Development*. 2016; 143: 2249-60.
5. Albini A, Tosetti F, Li VW, Noonan DM, Li WW. Cancer prevention by targeting angiogenesis. *Nat Rev Clin Oncol*. 2012; 9: 498-509.

6. Potente M, Gerhardt H, Carmeliet P. Basic and therapeutic aspects of angiogenesis. *Cell*. 2011; 146: 873-87.
7. Weavers H, Skaer H. Tip cells: master regulators of tubulogenesis? *Semin Cell Dev Biol*. 2014; 31: 91-9.
8. Ribatti D, Crivellato E. "Sprouting angiogenesis", a reappraisal. *Dev Biol*. 2012; 372: 157-65.
9. Xu G, Qi LN, Zhang MQ, Li XY, Chai JL, Zhang ZQ, et al. Galphai1/3 mediation of Akt-mTOR activation is important for RSPO3-induced angiogenesis. *Protein Cell*. 2023; 14: 217-22.
10. Shan HJ, Jiang K, Zhao MZ, Deng WJ, Cao WH, Li JJ, et al. SCF/c-Kit-activated signaling and angiogenesis require Galphai1 and Galphai3. *Int J Biol Sci*. 2023; 19: 1910-24.
11. Li Y, Chai JL, Shi X, Feng Y, Li JJ, Zhou LN, et al. Galphai1/3 mediate Netrin-1-CD146-activated signaling and angiogenesis. *Theranostics*. 2023; 13: 2319-36.
12. Yao J, Wu XY, Yu Q, Yang SF, Yuan J, Zhang ZQ, et al. The requirement of phosphoenolpyruvate carboxykinase 1 for angiogenesis in vitro and in vivo. *Sci Adv*. 2022; 8: eabn6928.
13. Sun J, Huang W, Yang SF, Zhang XP, Yu Q, Zhang ZQ, et al. Galphai1 and Galphai3 mediate VEGF-induced VEGFR2 endocytosis, signaling and angiogenesis. *Theranostics*. 2018; 8: 4695-709.
14. Villaseca S, Romero G, Ruiz MJ, Perez C, Leal JL, Tovar LM, et al. Galphai protein subunit: A step toward understanding its non-canonical mechanisms. *Front Cell Dev Biol*. 2022; 10: 941870.
15. Gupta V, Bhandari D, Leyme A, Aznar N, Midde KK, Lo IC, et al. GIV/Girdin activates Galphai and inhibits Galphas via the same motif. *Proc Natl Acad Sci U S A*. 2016; 113: E5721-30.
16. Nishida M, Schey KL, Takagahara S, Kontani K, Katada T, Urano Y, et al. Activation mechanism of Gi and Go by reactive oxygen species. *J Biol Chem*. 2002; 277: 9036-42.
17. McCudden CR, Hains MD, Kimple RJ, Siderovski DP, Willard FS. G-protein signaling: back to the future. *Cell Mol Life Sci*. 2005; 62: 551-77.
18. Wiege K, Ali SR, Gewecke B, Novakovic A, Konrad FM, Pexa K, et al. Galphai2 is the essential Galphai protein in immune complex-induced lung disease. *J Immunol*. 2013; 190: 324-33.
19. Milligan G, Kostenis E. Heterotrimeric G-proteins: a short history. *Br J Pharmacol*. 2006; 147 Suppl 1: S46-55.
20. Cao C, Huang X, Han Y, Wan Y, Birnbaumer L, Feng GS, et al. Galpha(i1) and Galpha(i3) are required for epidermal growth factor-mediated activation of the Akt-mTORC1 pathway. *Sci Signal*. 2009; 2: ra17.
21. Wang Y, Liu YY, Chen MB, Cheng KW, Qi LN, Zhang ZQ, et al. Neuronal-driven glioma growth requires Galphai1 and Galphai3. *Theranostics*. 2021; 11: 8535-49.
22. Marshall J, Zhou XZ, Chen G, Yang SQ, Li Y, Wang Y, et al. Antidepressant action of BDNF requires and is mimicked by Galphai1/3 expression in the hippocampus. *Proc Natl Acad Sci U S A*. 2018; 115: E3549-E58.
23. Zhang YM, Zhang ZQ, Liu YY, Zhou X, Shi XH, Jiang Q, et al. Requirement of Galphai1/3-Gab1 signaling complex for keratinocyte growth factor-induced PI3K-AKT-mTORC1 activation. *J Invest Dermatol*. 2015; 135: 181-91.
24. Li X, Wang D, Chen Z, Lu E, Wang Z, Duan J, et al. Galphai1 and Galphai3 regulate macrophage polarization by forming a complex containing CD14 and Gab1. *Proc Natl Acad Sci U S A*. 2015; 112: 4731-6.
25. Bai JY, Li Y, Xue GH, Li KR, Zheng YF, Zhang ZQ, et al. Requirement of Galphai1 and Galphai3 in interleukin-4-induced signaling, macrophage M2 polarization and allergic asthma response. *Theranostics*. 2021; 11: 4894-909.
26. Wang Y, Liu F, Wu J, Zhang MQ, Chai JL, Cao C. G protein inhibitory alpha subunit 2 is a molecular oncotarget of human glioma. *Int J Biol Sci*. 2023; 19: 865-79.
27. Chen M, Li Z, Gu C, Zheng H, Chen Y, Cheng L. Identification of G protein subunit alpha i2 as a promising therapeutic target of hepatocellular carcinoma. *Cell Death Dis*. 2023; 14: 143.
28. Slepak VZ, Katz A, Simon MI. Functional analysis of a dominant negative mutant of G alpha i2. *J Biol Chem*. 1995; 270: 4037-41.
29. Zhang XP, Li KR, Yu Q, Yao MD, Ge HM, Li XM, et al. Ginsenoside Rh2 inhibits vascular endothelial growth factor-induced corneal neovascularization. *FASEB J*. 2018; 32: 3782-91.
30. Gao YY, Ling ZY, Zhu YR, Shi C, Wang Y, Zhang XY, et al. The histone acetyltransferase HBO1 functions as a novel oncogenic gene in osteosarcoma. *Theranostics*. 2021; 11: 4599-615.
31. Liu TT, Shi X, Hu HW, Chen JP, Jiang Q, Zhen YF, et al. Endothelial cell-derived RSPO3 activates Galphai1/3-Erk signaling and protects neurons from ischemia/reperfusion injury. *Cell Death Dis*. 2023; 14: 654.
32. Shao NY, Wang DX, Wang Y, Li Y, Zhang ZQ, Jiang Q, et al. MicroRNA-29a-3p Downregulation Causes Gab1 Upregulation to Promote Glioma Cell Proliferation. *Cell Physiol Biochem*. 2018; 48: 450-60.
33. Cao C, Rioult-Pedotti MS, Migani P, Yu CJ, Tiwari R, Parang K, et al. Impairment of TrkB-PSD-95 signaling in Angelman syndrome. *PLoS Biol*. 2013; 11: e1001478.
34. Xu G, Qi L-n, Zhang M-q, Li X-y, Chai J-l, Zhang Z-q, et al.  $\alpha$ i1/3 mediation of Akt-mTOR activation is important for RSPO3-induced angiogenesis. *Protein & Cell*. 2022.
35. Scott A, Fruttiger M. Oxygen-induced retinopathy: a model for vascular pathology in the retina. *Eye (Lond)*. 2010; 24: 416-21.
36. Connor KM, Krah NM, Dennison RJ, Aderman CM, Chen J, Guerin KI, et al. Quantification of oxygen-induced retinopathy in the mouse: a model of vessel loss, vessel regrowth and pathological angiogenesis. *Nat Protoc*. 2009; 4: 1565-73.
37. Salvioi S, Ardizzoni A, Franceschi C, Cossarizza A. JC-1, but not DiOC6(3) or rhodamine 123, is a reliable fluorescent probe to assess delta psi changes in intact cells: implications for studies on mitochondrial functionality during apoptosis. *FEBS Lett*. 1997; 411: 77-82.
38. Minetti GC, Feige JN, Rosenstiel A, Bombard F, Meier V, Werner A, et al. Galphai2 signaling promotes skeletal muscle hypertrophy, myoblast differentiation, and muscle regeneration. *Sci Signal*. 2011; 4: ra80.
39. Hernandez GL, Volpert OV, Iniguez MA, Lorenzo E, Martinez-Martinez S, Grau R, et al. Selective inhibition of vascular endothelial growth factor-mediated angiogenesis by cyclosporin A: roles of the nuclear factor of activated T cells and cyclooxygenase 2. *J Exp Med*. 2001; 193: 607-20.
40. Suehiro J, Kanki Y, Makihara C, Schadler K, Miura M, Manabe Y, et al. Genome-wide approaches reveal functional vascular endothelial growth factor (VEGF)-inducible nuclear factor of activated T cells (NFAT) c1 binding to angiogenesis-related genes in the endothelium. *J Biol Chem*. 2014; 289: 29044-59.
41. Suehiro J, Hamakubo T, Kodama T, Aird WC, Minami T. Vascular endothelial growth factor activation of endothelial cells is mediated by early growth response-3. *Blood*. 2010; 115: 2520-32.
42. Han C, Nie S, Chen G, Ma K, Xiong N, Zhang Z, et al. Intrastriatal injection of ionomycin profoundly changes motor response to L-DOPA and its underlying molecular mechanisms. *Neuroscience*. 2017; 340: 23-33.
43. Hawkshaw NJ, Paus R. Beyond the NFAT Horizon: From Cyclosporine A-Induced Adverse Skin Effects to Novel Therapeutics. *Trends Pharmacol Sci*. 2021; 42: 316-28.
44. Kawahara T, Kashiwagi E, Li Y, Zheng Y, Miyamoto Y, Netto GJ, et al. Cyclosporine A and tacrolimus inhibit urothelial tumorigenesis. *Mol Carcinog*. 2016; 55: 161-9.
45. Slepak VZ, Quick MW, Aragay AM, Davidson N, Lester HA, Simon MI. Random mutagenesis of G protein alpha subunit G(o)alpha. Mutations altering nucleotide binding. *J Biol Chem*. 1993; 268: 21889-94.
46. Ma ZR, Li HP, Cai SZ, Du SY, Chen X, Yao J, et al. The mitochondrial protein TIMM44 is required for angiogenesis in vitro and in vivo. *Cell Death Dis*. 2023; 14: 307.
47. Al-Latayfeh M, Silva PS, Sun JK, Aiello LP. Antiangiogenic therapy for ischemic retinopathies. *Cold Spring Harb Perspect Med*. 2012; 2: a006411.
48. Wang W, Lo ACY. Diabetic Retinopathy: Pathophysiology and Treatments. *Int J Mol Sci*. 2018; 19.
49. Stitt AW, Curtis TM, Chen M, Medina RJ, McKay GJ, Jenkins A, et al. The progress in understanding and treatment of diabetic retinopathy. *Prog Retin Eye Res*. 2016; 51: 156-86.
50. Capitaio M, Soares R. Angiogenesis and Inflammation Crosstalk in Diabetic Retinopathy. *J Cell Biochem*. 2016; 117: 2443-53.
51. Salam A, Mathew R, Sivaprasad S. Treatment of proliferative diabetic retinopathy with anti-VEGF agents. *Acta Ophthalmol*. 2011; 89: 405-11.
52. Jardeleza MS, Miller JW. Review of anti-VEGF therapy in proliferative diabetic retinopathy. *Semin Ophthalmol*. 2009; 24: 87-92.
53. Abdallah W, Fawzi AA. Anti-VEGF therapy in proliferative diabetic retinopathy. *Int Ophthalmol Clin*. 2009; 49: 95-107.
54. Park YJ, Yoo SA, Kim M, Kim WU. The Role of Calcium-Calcineurin-NFAT Signaling Pathway in Health and Autoimmune Diseases. *Front Immunol*. 2020; 11: 195.
55. Fric J, Zelante T, Wong AY, Mertes A, Yu HB, Ricciardi-Castagnoli P. NFAT control of innate immunity. *Blood*. 2012; 120: 1380-9.
56. Nguyen T, Di Giovanni S. NFAT signaling in neural development and axon growth. *Int J Dev Neurosci*. 2008; 26: 141-5.
57. Buchholz M, Ellenrieder V. An emerging role for Ca2+/calcineurin/NFAT signaling in cancerogenesis. *Cell Cycle*. 2007; 6: 16-9.
58. Schulz RA, Yutzey KE. Calcineurin signaling and NFAT activation in cardiovascular and skeletal muscle development. *Dev Biol*. 2004; 266: 1-16.
59. Armesilla AL, Lorenzo E, Gomez del Arco P, Martinez-Martinez S, Alfranca A, Redondo JM. Vascular endothelial growth factor activates nuclear factor of activated T cells in human endothelial cells: a role for tissue factor gene expression. *Mol Cell Biol*. 1999; 19: 2032-43.



60. Bahrami B, Hong T, Gilles MC, Chang A. Anti-VEGF Therapy for Diabetic Eye Diseases. *Asia Pac J Ophthalmol (Phila)*. 2017; 6: 535-45.
61. Krick TW, Bressler NM. Recent clinically relevant highlights from the Diabetic Retinopathy Clinical Research Network. *Curr Opin Ophthalmol*. 2018; 29: 199-205.
62. Tremolada G, Del Turco C, Lattanzio R, Maestroni S, Maestroni A, Bandello F, *et al*. The role of angiogenesis in the development of proliferative diabetic retinopathy: impact of intravitreal anti-VEGF treatment. *Exp Diabetes Res*. 2012; 2012: 728325.
63. Osaadon P, Fagan XJ, Lifshitz T, Levy J. A review of anti-VEGF agents for proliferative diabetic retinopathy. *Eye (Lond)*. 2014; 28: 510-20.